NATIONAL ADVISORY COMMITTEE FOR AERONAUTICS

TECHNICAL NOTE

No. 1320

INVESTIGATION OF THE DYNAMIC RESPONSE OF AIRPLANE WINGS TO GUSTS

By Harold B. Pierce

Langley Memorial Aeronautical Laboratory
Langley Field, Va.

Washington
June 1947

E R R A T A

NACA TN No. 1320

INVESTIGATION OF THE DYNAMIC RESPONSE
OF AIRPLANE WINGS TO GUSTS
By Harold B. Pierce
June 1947

Page 29: Equation (A6) should read as follows:

$$\delta_f = c_1 e^{R_1 t} (\cos R_2 t) + c_2 e^{R_1 t} (\sin R_2 t) + c_3 e^{R_3 t}$$

$$+ c_4 + \frac{F_1}{G_1} t e^{-bt} + \left(\frac{F_2}{G_1} + \frac{F_1 G_2}{G_1^2} \right) e^{-bt}$$

Page 31: The last term of equation (All) should be

$$- \frac{A_c b}{\lambda_c - b} t e^{-bt}$$

NATIONAL ADVISORY COMMITTEE FOR AERONAUTICS

TECHNICAL NOTE NO. 1320

INVESTIGATION OF THE DYNAMIC RESPONSE OF AIRPLANE WINGS TO GUSTS

By Harold B. Pierce

SUMMARY

A method of predicting the dynamic response of airplane wings to gusts by considering only the fundamental mode of bending is presented, together with the results of model tests made to evaluate the method. In addition, the results of a series of calculations obtained by using the method are given to illustrate changes in the dynamic response of airplane wings brought about by changes in gust and airplane parameters. An appendix giving the details of the method and the procedure for the determination of constants is included.

Although the test results are not suitable for predicting dynamic-stress ratios, they serve to indicate that the method is of sufficient accuracy to predict the ratio of maximum dynamic wing deflection to maximum fuselage acceleration increment for conventional airplanes. The test results also illustrate the need for including aerodynamic damping in calculations of dynamic response of airplane wings.

The calculations made to show the effect of change of certain gust parameters indicate that:

(1) The dynamic-stress ratio for airplane wings increases as the gradient distance of the gust decreases.

(2) For the assumed design gust of 10-chord gradient distance, the overstress in a single gust may be as much as 12 percent.

(3) Although the results for one type of repeated gust are not conclusive, a repeated gust does not seem to be more critical than a single gust.

The calculations made to show the effect of change of certain airplane parameters indicate that for the assumed design gust of 10-chord gradient distance:

(1) A change in forward velocity of the airplane does not appreciably change the dynamic-stress ratio.

(2) A reduction of wing frequency by a change either in weight or in stiffness of the wing results in an increase in the dynamic-stress ratio.

(3) The wing-tip acceleration increment is generally much greater than the fuselage acceleration increment and the ratio of the two tends to increase as the speed increases.

INTRODUCTION

In the present-day design of airplane wings for strength, the predominating loads considered are caused by maneuvering and by gusts. For transport-type airplanes, for which the design maneuvering loads are relatively low, the design gust loads are frequently critical, especially as the operating speed increases. These gust loads, for simplicity of calculation, are assumed to be static loads applied to a rigid airplane. For the smaller airplanes, the assumption of a rigid structure appears to be reasonable. With increase in size, however, airplane wings tend to deflect more and, thus, the assumption of rigidity is subject to question. Consequently, the trend toward larger and faster airplanes necessitates the determination of methods for calculating and evaluating the effects of dynamic response.

In the past a number of investigations of the dynamic response of airplane wings on encountering gusts have been conducted. Notable among these investigations are the ones reported in references 1 to 4. In reference 1, under the assumption of no pitching motion, Küssner sets forth the exact equations for the loads and moments when the airplane encounters a gust and applies these equations to the flexural system which is composed of the wing and fuselage of an airplane. Since a mathematical error was found in his simplification of these integro-differential equations, the calculated results given by Küssner are therefore considered invalid. References 2 and 3 present two other simplifications of the problem, but the dynamic-stress results are difficult to dissociate from the stability reactions in which they are contained.

Reference 4 presents still another simplification that is based on an infinite-mass fuselage. These reference papers represent isolated investigations of various parameters affecting the dynamic response of airplanes to gusts and use a number of methods that cannot readily be evaluated by comparison. In addition, the validity of the various investigations has never been experimentally shown.

Upon consideration of the need for investigating the flexural reactions of large airplanes in gusts and because of the omissions in the existing literature, an investigation was undertaken with the following purposes in mind:

(1) To evolve a relatively simple, yet sufficiently accurate method for determining the dynamic stress in the wings of a given airplane due to their dynamic response to gusts.

(2) To make an experimental check of the method.

(3) To make a study of the effect of the changes of gust and airplane parameters on the stress due to the dynamic response of airplane wings.

The results of this investigation are presented herein, together with the analytical method, which is restricted to the fundamental mode of bending and includes aerodynamic damping.

SYMBOLS

M_{w_e}	equivalent mass of wing, slugs
M_{f_e}	equivalent mass of wing-fuselage, slugs
M	mass of airplane, slugs, $\left(M_{w_e} + M_{f_e}\right)$
δ_w	absolute displacement of equivalent wing, feet
δ_f	absolute displacement of equivalent wing-fuselage, feet
δ_d	wing-tip deflection increment, feet, $(\delta_w - \delta_f)$

$\delta_{d_{max}}$	maximum value of $(\delta_w - \delta_f)$, feet
δ_{st}	deflection of equivalent wing under conditions corresponding to normal static design procedure, feet
λ_{w_e}	equivalent wing damping coefficient, pound-seconds per foot
λ_{f_e}	equivalent wing-fuselage damping coefficient, pound-seconds per foot
λ	damping coefficient of entire airplane, pound-seconds per foot, $\left(\lambda_{w_e} + \lambda_{f_e}\right)$
K	equivalent spring constant based on wing frequency and equivalent wing mass, pounds per foot
f	wing frequency, cycles per second
t	time, seconds
F(t)	forcing function on entire airplane, pounds
$F_{w_e}(t)$	forcing function on equivalent wing, pounds
$F_{f_e}(t)$	forcing function on equivalent wing-fuselage, pounds
Δn	acceleration increment normal to chord of wing, g units
Δn_r	acceleration increment on rigid airplane, g units
$\Delta n_{r_{max}}$	maximum value of acceleration increment on rigid airplane, g units
L_1	proportion of total air load assumed to deflect equivalent wing
W	weight of airplane and of equivalent biplane, pounds
W_{w_e}	weight of equivalent wing, pounds
U	gust velocity, feet per second
$U_{max_{av}}$	average maximum gust velocity, feet per second
$\Delta\theta$	pitch-angle increment, degrees

V forward velocity, feet per second

D differential operator

H_1 gradient distance of the first gust (fig. 2), chords

H_2 gradient distance of the second gust (fig. 2), chords

H_3 distance between the end of the gradient distance of first gust and the beginning of the gradient distance of second gust (fig. 2), chords

$A = \frac{\Delta n_a W}{te^{-bt}}$ at $bt = 1$

$= Wbe\Delta n_a$

Δn_a arbitrary load-factor increment that the airplane would experience if it had no vertical motion when traversing the gust, g units

$b = \frac{1}{t}$ at $bt = 1$ or at the maximum value of the function te^{-bt}

ANALYTICAL METHOD

Examination of the problem of the dynamic response of airplanes to gusts shows that the spanwise distribution of the imposed loads varies over wide limits (reference 5) and that the structure itself may react in a number of combinations of modes. Rather than attempt to solve the general case, consideration was given to a method for determining the origin of the principal stresses with the intention of reducing the problem to one of reasonable dimensions. As a result, this paper is concerned with the analysis of the fundamental mode of bending of the wing under symmetrical loads which are assumed to be known.

Development of Method

Briefly, the present method follows the steps given in references 2 and 3 in that the airplane is replaced by a simple equivalent aerodynamic and elastic system. The basic forms of forcing function to be used for the response of an airplane to known single gusts, however, have been selected from the results of gust-tunnel tests such as those described in reference 6.

Biplane as equivalent airplane.- The problem of determining the stress caused by dynamic response is simplified by the previous assumption that the fundamental mode of vibration of the wing is the most significant. As a result, the deflection of the wing tip with respect to the fuselage may be taken as a direct measure of the stress in the wing. The equivalent system, then, is represented as a biplane (fig. 1) that has the motions of the rigid upper wing and the rigid lower wing-fuselage combination adjusted to have the same motions as the wing tip and fuselage of the airplane under investigation. The equivalent biplane system must include the proper distribution of aerodynamic as well as inertia and elastic forces or force coefficients. The problem is then resolved into one of obtaining the proper constants to be used as coefficients in simultaneous linear differential equations which represent the equivalent biplane. These equations follow:

$$M_{w_e} \frac{d^2\delta_w}{dt^2} + \lambda_{w_e} \frac{d\delta_w}{dt} + K(\delta_w - \delta_f) = F_{w_e}(t) \qquad (1)$$

$$M_{f_e} \frac{d^2\delta_f}{dt^2} + \lambda_{f_e} \frac{d\delta_f}{dt} - K(\delta_w - \delta_f) = F_{f_e}(t) \qquad (2)$$

These equations are solved for the stress in the wing as represented by the wing deflection $(\delta_w - \delta_f)$ and for the load parameters represented by the fuselage and wing-tip acceleration increments. The details of the solution and the procedure for determination of the coefficients are given in the appendix.

Since the normal gust-load design procedure assumes that the load is applied statically and that the normal acceleration is constant along the span of the airplane, the dynamic wing deflection must be compared with the static wing deflection under the action of the acceleration of the "rigid" airplane. In order that the comparison be valid, the rigid-airplane acceleration Δn_1 is determined as the response of the equivalent biplane to the sum of the forcing functions $F_{w_e}(t)$ and $F_{f_e}(t)$ when the springs are replaced by

rigid rods. The static deflection δ_{st} is then calculated from the simple formula

$$\delta_{st} = \frac{\Delta n_{r_{max}} \left(L_1 W - W_{w_e}\right)}{K} \tag{3}$$

which, in accordance with normal design procedure, considers no aerodynamic damping of the static wing deflection. The stress computed by the static-load method is therefore multiplied by the ratio $\delta_{d_{max}}/\delta_{st}$.

Of further interest is the fact that, since equations 1 and 2 are linear, ratios of the maximum flexible-wing acceleration increments to the corresponding maximum rigid-airplane acceleration increments are independent of the magnitude of the load and may be applied directly as multiplying factors to those acceleration increments computed in the determination of the gust load.

Required conditions.- In arriving at the characteristic values of the coefficients for the equivalent biplane, the following conditions should be satisfied:

(1) The total mass of and the total load on the equivalent biplane should be identical with those of the original airplane.

(2) The kinetic energy of vibration of the upper wing should closely approximate that of the original wing beam for an amplitude of vibration of the upper wing equal to that of the tip of the original wing.

(3) The natural frequency should be the same as that for the fundamental mode of the original wing.

(4) The upper wing should deflect under the equivalent static load the same amount that the wing tip of the airplane does under the corresponding aerodynamic static-load distribution.

(5) The damping coefficient of the upper wing should represent, at least to peak load, the damping of the motion of the wing.

Discussion of Terms

Equivalent masses and spring constant.- The equivalent masses and spring constant are determined from conditions (1) to (3). The equivalent mass of the wing M_{w_e} is generally determined

first and the equivalent spring constant K is then determined from the known or estimated wing frequency. The equivalent wing-fuselage mass M_{f_e} is then simply the total mass of the airplane M minus M_{w_e}. For special cases, such as strut-supported wings and arrangements other than the conventional cantilever monoplane, considerable care is required.

Damping coefficient.- The damping coefficient is actually the lift per unit vertical velocity for each wing section along the span of the airplane and, as such, includes the effect of the vertical motion of the airplane as a whole, as well as that of the vibratory velocity caused by the bending action of the wing. Although the lift or damping force arising from the two motions would be subject to the effects of unsteady flow, an analysis and some tests, described in the appendix, indicate that an acceptable approximation to the unsteady-lift damping load is to represent this load as 75 percent of the steady-lift damping load. The proportion of the total damping coefficient assigned to the upper wing of the equivalent biplane should change as the airplane traverses the gust because of the change in the relative significance of the wing-deflection velocity and the vertical velocity of the airplane as a whole. In a given calculation, however, the proportion used is assumed to be determined by the relation existing between the velocities at the time of maximum wing deflection. Since this relation is not known prior to the calculations, an approximate criterion, described in the appendix, was determined for the division of the total damping coefficient λ into λ_{w_e} and λ_{f_e}.

Forcing functions.- The forcing function is considered to be the time history of the air loads applied to the rigid airplane minus the damping load due to vertical motion. The omission of the damping load due to vertical motion from the total air loads is necessary because it is included in the damping terms of equations (1) and (2), which provide for approximation of both the vertical motion and vibratory damping. With this omission in mind, the forcing function may be determined by any of several available methods. One method used by Küssner (reference 1) is to set up the basic equations in terms of gust velocity and its spanwise distribution and to include these equations directly as the forcing functions in equations (1) and (2). A second method would be to solve a set of equations such as given in reference 7, which describe the reaction of a rigid airplane to a gust and, from the resulting time history of acceleration, to determine a curve representing the forcing function F(t). In order to permit this second form of the forcing function to be used readily, a solution

is made of equations (1) and (2) with a unit-function type of forcing function (reference 8) for a desired reaction such as wing deflection. The results are then combined through the use of Duhamel's integral which may be solved graphically through use of the method given in reference 9.

Since for these calculations the shape of the curve representing the forcing function is the principal characteristic and since the unsteady-lift effects and the effects caused by stability reactions are of doubtful accuracy insofar as their predictions are concerned, it seemed desirable to make some approximation of the forcing function to obviate its calculation for each airplane. This approximation was accomplished through the analysis of accelerometer records from the tests of rigid-airplane models traversing known gusts of the type shown in figure 2(a). The procedure followed was to compute the time history of the vertical velocity during the traverse of the gust, to determine the damping force due to this vertical velocity, and to add the acceleration increment due to this damping force to the net acceleration increment from passage through the gust. For representative gust shapes, from a sharp-edge gust to one rising to maximum velocity in 20 chords, the resulting time histories of the forcing functions were determined and it was found that, for practical purposes, all curves could be represented by a function of the type Ate^{-bt}. When unconventional designs are considered, however, it appears that the second method mentioned or tests of the model in the gust tunnel should be used to determine the forcing-function type.

The specific shape of the curve representing the forcing function Ate^{-bt} for a given calculation is determined from an approximate relationship between the chordwise velocity distribution of the chosen gust and the reaction of the given airplane to the forcing function. The tests on rigid-airplane models also showed that the maximum value of acceleration increment occurs approximately at the time that the model reaches the end of the gust gradient distance H_1. As a result, the choice of the value b in the forcing function Ate^{-bt} to make this forcing function represent a given gust gradient distance is merely one of making the time history of the rigid-airplane acceleration increment Δn_r reach its maximum value at the same time that the airplane reaches the end of the gust gradient distance H_1. A general procedure for the selection of values of b to represent given gusts is outlined in the appendix.

The forcing function $F_{w_e}(t)$ is ascertained by determining the equivalent static load on the upper wing of the equivalent biplane which would yield the same deflection of the upper wing as the total distributed static air load yields for the original wing tip. The forcing function $F_{f_e}(t)$ is then merely the difference between $F(t)$ and $F_{w_e}(t)$.

EXPERIMENTAL INVESTIGATION

In order to obtain information on the reliability of dynamic response calculations of the type considered herein and the difficulties to be expected in any actual application, tests were made in the gust tunnel of a simple model equipped with semirigid wings. These tests were conducted for three conditions of wing stiffness and for three gust-gradient distances to determine the fuselage acceleration and the corresponding wing-tip deflection increments.

Apparatus

The model used for the tests is shown in figure 3. Pertinent characteristics of the model are given in table I and in figure 4. The wing panels were rigid and connected to the cabane by flexure plates to permit freedom of motion in "bending" while offering a maximum stiffness in torsion. Struts connected by universal joints to the wing (fig. 5) were supported on the inboard end by cantilever springs which could easily be changed to modify the natural wing frequency. The rigid-wing condition was obtained by attaching the struts directly to the fuselage.

The model carried a miniature accelerometer and lights at the nose and tail and other lights were located at the wing-strut connections to impress records of the wing-tip deflection on the accelerometer film through a lens mirror system as indicated in figure 6. A sample accelerometer record is shown in figure 7 where the time histories of wing-tip deflection are labeled A and the acceleration time history is labeled B. The distance C between the time histories results from the fact that the two record light beams strike the film 90° apart on the drum.

The gust tunnel and associated equipment have been described in detail in reference 6. The gust types pertinent to the present paper are shown, together with test results subsequently described, in figures 8 to 10.

Tests

Tests consisted of a minimum of 10 flights for each of the wing-frequency values, 13.5, 26.1, and infinite cycles per second, and related spring constants and for each of three gust types. The tests were made for one forward velocity, gust velocity, and airplane weight so that the only variables were gust type and wing frequency. For each flight of the model through the gust, measurements were made of the forward velocity, gust velocity, normal fuselage acceleration, wing-tip deflection, and the pitching motion.

Precision

The measured quantities are estimated to be accurate within the following limits for any flight:

Normal fuselage acceleration increment, g units	±0.05
Wing-tip deflection, inches	±0.01
Forward velocity, feet per second	±1.0
Gust velocity, feet per second	±0.1
Pitch-angle increment, degrees	±0.2

In addition to errors in the recorded quantities resulting from instrument characteristics and limitations on reading accuracy, another error which is difficult to evaluate is that of the uniformity of the gust shape both laterally and longitudinally. The longitudinal variation (in the direction of flight) of the gust shapes shown in figures 8 to 10 would tend to modify the shape of curve representing the forcing function from that assumed for a linear gradient. With such variations existing in the direction of flight similar variations might exist across the span of the model. Inspection of more recent surveys taken 1 foot on either side of the center line indicate that, at points in the gust, such variations could be of the order of 12 percent of the center value.

Results

The launching is intended to set the model in a steady straight glide at constant speed without pitch, roll, or yaw. In actual tests the fulfillment of these ideal conditions is almost impossible and therefore, all flights in which pitch, roll, or yaw were excessive prior to entry into the gust must be disregarded. The records from each satisfactory flight were evaluated to obtain time histories of acceleration increment, wing-tip deflection increment, and pitch

increment during the entire traverse of the gust and to obtain the forward speed and gust velocity for the flight. Sample time histories of the acceleration increment and the wing-tip deflection increment are shown in figures 8 and 9 for the two wing frequencies used, 13.5 and 26.1 cycles per second, respectively, and the time histories of acceleration increment are shown in figure 10 for the rigid-wing condition. The results are plotted against the distance penetrated into the gust in chords and have been corrected to a forward speed of 61 feet per second and a gust velocity of 6 feet per second on the assumption that the acceleration increment and wing-tip deflection increment are directly proportional to forward speed and gust velocity for small variations in these quantities. Results for two flights under similar conditions are shown as a sample of the data obtained for each condition of wing stiffness and gust shape.

In order to provide a measure of the pitching response of the airplane model, data are presented giving the pitch-increment ratio $\frac{\Delta\theta/57.3}{U/V}$ at the instant of maximum acceleration increment. Analysis of past gust-tunnel tests has shown that this ratio is approximately equal to the fraction by which the measured acceleration increment differs from that predicted by the analysis of reference 10, which assumes that the airplane does not pitch while traversing a gust. Average values of $\frac{\Delta\theta/57.3}{U/V}$ for each test condition are shown in figure 11 as a function of the distance to peak acceleration increment to indicate the dependence of the ratio on gust gradient distance. Also shown is the scatter band of data for four models (six conditions of weight and speed) from the tests of which the forcing function Ate^{-bt} was derived.

Figure 12 shows the maximum values of acceleration and wing-tip deflection increments for each wing frequency, for all records read, as the wing-tip deflection per unit acceleration plotted against the gradient distance. The right and left wing results have been given separately to show the degree of symmetry of the wing-tip deflections.

CALCULATIONS

In the preceding sections of this report, a method was outlined for calculating the dynamic response of airplane wings under the action of arbitrary gusts and some simple tests of a model in the

gust tunnel were described. The remaining problems are to determine whether, considering the experimental data, the method yields results of reasonable accuracy and, finally, to investigate in a general way some of the significant factors which determine the degree of dynamic response of airplane wings in turbulent air.

The first problem - that of checking the accuracy of the method against experimental data - may be solved simply by checking the data obtained for the airplane model against calculations based on the conditions for which the tests were made. Data for the solution of the second problem, however, requires calculations for representative airplanes for which dynamic response might be of some concern. The airplanes selected for these calculations were those for which some information as to structure and mass distribution was available.

Briefly, the calculations were made to indicate the effects of airplane weight, weight distribution, gust size, airplane speed, and wing stiffness and to investigate the possibility of further simplification in the method of calculation.

Calculations for Comparison with Experimental Results

In the dynamic-stress calculations for the test model the principal differences from the method set forth in this paper for the normal cantilever-wing airplane arise from the fact that the wings of the model deflect about the hinge as rigid bodies. As a result, parameters affecting angular-frequency reactions predominate. In other words, the actual spring constant of the model is in units of torque per degree of deflection and the reactions of the wing also depend on the moment of inertia of the wing panels about the hinge point. The moment of inertia of the wing panels, therefore, was determined experimentally and the equivalent wing mass for the calculations was that mass which, if placed at the model wing tip, would have the same moment of inertia about the hinge points as the wing panels. Since the wing frequencies for the two model conditions were known, the equivalent linear spring constants were then determined.

Further differences from the normal cantilever-wing case arise when consideration is given to the division of the air and damping loads applied to the model into the corresponding loads for the equivalent biplane. The division of the damping coefficient in the sharp-edge gust and in the gust with 10-chord gradient distance can be shown to be approximately 0.50 and 0.50 for the equivalent

wing and wing-fuselage, respectively, whereas for gradient distances greater than 10 chords the division approximates that for the air load, namely, 0.37 and 0.63 for the wing and wing-fuselage.

The equivalent constants, together with the values such as test forward velocity and the gradient distances of the test gusts, are included in table I. The actual gust profiles $\left(U/U_{max_{av}}\right.$ plotted against horizontal distance from edge of gust tunnel$\left.\right)$ are given in figures 8 to 10. In the case of the sharp-edge gust, the value of b, chosen for the forcing function Ate^{-bt}, was determined from the average of values of the time required to obtain peak acceleration of the model in the rigid-wing condition on entering this type of gust and corresponds to 4.6 chords of travel into the gust since, in this problem, the lag in development of lift of a wing entering such a gust has the effect of a gust with short gradient distance.

Calculations for the model with an arbitrary impressed load corresponding to a Δn_a of $2g$ were then made to determine time histories of wing-tip acceleration increment, fuselage acceleration increment, and wing-tip deflection increment for the conditions given in table I. The shapes of the calculated time-history curves of fuselage acceleration increment were compared with the experimental curves for each flight by adjusting the maximum calculated value to agree with the maximum experimental value. By using as the adjusting factor the ratio of maximum calculated to experimental values of fuselage acceleration increment for each flight, the calculated time histories of wing-tip deflection increment were then compared with the experimental time histories. Sample comparisons are given in figures 13 to 15. Included in figures 13 and 14 is a line representing the calculated value of the static deflection δ_{st} for each condition shown. The calculated wing-tip deflection per g of fuselage acceleration increment for each condition is compared with the test results in figure 12.

Additional calculations for the two flexible conditions of the model were made under the assumption of no vibratory damping. The method used for these calculations was obtained by eliminating the damping terms from the left-hand sides of equations (1) and (2) and by using net forcing functions which included the damping of the vertical motion of the airplane as a whole. The results of these calculations are also presented in figure 12 as the wing-tip deflection per g of acceleration increment.

Calculations for Effect of Change of Certain Parameters on Dynamic Response

The airplanes chosen for the calculations are designated models A, B, C, and D: model A is a scaled-up version of the test model which may be considered to represent a four-engine landplane, models B and C are four-engine landplanes, and model D is a large bimotored flying boat. Some of the data for models C and D have been presented previously in reference 11 but have been included herein for purposes of further analysis.

The changes in airplane constants chosen for consideration were those resulting from the effects of varying the wing stiffness, of arbitrarily omitting all vibratory damping and fuselage damping alone, and of varying the flight conditions of forward velocity and weight. The conditions and basic constants for the calculations are included in tables II and III.

General conditions.- The chordwise velocity distribution of a single gust was assumed to be of the type shown in figure 2(a). In almost all cases the calculations were made for three gust shapes, 0-, 10-, and about 20-chord gradient distance, although flight experience has shown that, for all sizes of modern airplanes, the most probable severe gust has a gradient distance of 10 chords. In all cases the forcing function representing the gust was of the form Ate^{-bt}.

Calculations of the effect of repeated gusts were made for distributions of the type shown in figure 2(c) by the method of superposition indicated in reference 8, pages 42-43, and illustrated in figure 2. The values of H_1 and H_2 were those chosen for the calculations for single gusts and the value of H_3 was determined to produce the greatest wing-tip deflection for the combination of gusts.

The results of the calculations for each airplane are presented in the form of three ratios plotted against the gradient distance of the gust for which the calculations were made (fig. 16). The maximum acceleration increments of the fuselage and of the wing tip of the airplane in the flexible condition are given as ratios to the corresponding maximum acceleration increments when the airplane is considered as a rigid body and are called the fuselage acceleration ratio and the wing-tip acceleration ratio. The wing-tip deflection ratio or the dynamic-stress ratio $\delta_{d_{max}}/\delta_{st}$ is the ratio of the maximum dynamic wing-tip deflection $\delta_{d_{max}}$ to the static wing-tip

deflection δ_{st} which would be determined under static loading conditions or as defined previously in equation (3). The individual calculations are outlined in the following sections:

Model A.- Model A is the scaled-up version of the gust-tunnel model. The two conditions for calculation (tables II and III) differ in the same way as the two conditions for the gust-tunnel model; that is, the wing frequency for condition 1 is approximately half that of condition 2. The results of the calculations in ratio form are given in figure 16(a) and 16(b) and a comparison of the dynamic-stress ratios for the two conditions are shown plotted against gradient distance in figure 17.

Model B.- The calculations for model B were made primarily to investigate the effect of simplifying the calculations by eliminating the fuselage damping term from equation (2) while keeping all other constants identical. The results of the calculations for each condition are given in figure 16(c) and 16(d) and a comparison of the dynamic-stress ratios for the two conditions is given in figure 18.

Model C.- Model C is a modern, large, and fast landplane. Calculations were made for a range of gust gradient distances for the airplane flying at its cruising speed of 260 miles per hour and the results in ratio form are given in figure 16(e). Additional calculations were made for assumed speeds of 200, 300, and 400 miles per hour for the standard gust with gradient distance of 10 chords in order to determine the effect of forward velocity on the various ratios. The ratios determined, together with those for the gust with gradient distance of 10 chords at 260 miles per hour, are shown plotted against forward velocity in figure 19. The calculations for the three gradient distances at 260 miles per hour are used subsequently in obtaining the response to repeated gusts.

Model D.- The calculations for model D were made to show the effect on the ratios of a change in weight of the airplane such as to change the frequency of the fundamental mode of vibration of the wing beam. The two conditions shown in tables II and III for this airplane represent the normal gross weight and the overload gross weight. Note that the forward velocities for the two conditions are different. The results of the calculations are given in figure 16(f) and 16(g). A comparison of the dynamic-stress ratios for the two conditions is given in figure 20. As in the case of model C, these calculations were also used for the determination of the response to repeated gusts.

Repeated gusts.- The basic curves chosen for the extension of the calculations to determine the response to two successive gusts were the time histories of the reactions of model C, condition 1, and model D, conditions 1 and 2, (figs. 21 to 23). Sample time-history curves for a repeated gust, composed of two equal and opposite gusts of gradient distance of 10 chords arranged relative to one another to give maximum negative wing deflection, are given in figures 24 to 26.

Since the interest is primarily in dynamic stress rather than in accelerations, the calculated basic curves were superimposed to determine the maximum overstress from the combination of the reactions to two gusts. The maximum values of dynamic-stress ratio occurred when the repeat gust was negative with respect to the first gust and the sequence period or distance H_3 (see fig. 2) had a pronounced effect on the result. The maximum value of Δn_r occurring in the whole sequence was used to determine the static wing-tip deflection. Table IV presents selected cases which were the most serious of a number of combinations examined. In this table, the results refer to repeat gusts having the same velocities as the initial gusts.

DISCUSSION

Experimental Results and Associated Calculations

Experimental results.- It was intended to determine the dynamic-stress ratios $\delta_{d_{max}}/\delta_{st}$ directly from the test results of the two flexible and one rigid condition of the model. Examination of the test data showed, however, that the scatter of the data within an individual test condition precluded such a procedure. As a result, the relative magnitudes of the wing-tip deflection in the flexible condition were used for comparison with calculations and these magnitudes were determined as the ratio of the maximum wing-tip deflection to the maximum fuselage acceleration for a given flight of the model.

As previously pointed out, the experimental data were corrected for variation in forward velocity and gust velocity and, therefore, the results for a given gust shape and model condition theoretically should be equal. Examination of figures 8 and 9 shows, however, that this equality does not exist and that the scatter, say, in the left wing-tip deflections may be as great as 17 percent in even these selected cases. In addition, the maximum values of acceleration

increment for the rigid condition, from which the static wing-tip deflection δ_{st} would be determined, had large scatter. Since the overstress or understress in these cases would probably not exceed 20 percent, the experimental data is not sufficiently consistent to predict the dynamic-stress ratios $\delta_{d_{max}}/\delta_{st}$.

Although the experimental data as a whole does not appear to be sufficiently accurate to be used as a check of the prediction of the dynamic-stress and acceleration ratios by the analytical method, the data in the form given in figure 12 appears to be sufficiently consistent to check the order of magnitude of the predicted wing-tip deflection. This experimental data in figure 12 is presented as the ratio of maximum wing-tip deflection to maximum measured acceleration increment as a function of the gradient distance of the imposed gust. The data for the right wing appeared to be less accurate than that for the left wing, probably because of local buckling of the right-wing hinge. The test data for the left wing then appears to be sufficiently consistent for use as a check of the order of magnitude of the predicted wing deflections.

Comparison of calculated results with experimental results.- The calculated results for the test model, represented by solid lines, are compared with the experimental results in figure 12. The comparison indicates that, for the consistent experimental data for the left wing, experiment and calculation are in good agreement as to the magnitude of the deflections.

Although figure 12 shows that the results for the left wing in the model condition of $f = 26.1$ cycles per second for the longest gradient distance differ by about 15 percent, this apparent disagreement is minimized by consideration of the precision of measurement of the experimental data. Examination of figure 14(c) shows that the recorded wing-tip deflection was only of the order of 0.07 inches. Since the precision of measurement is ± 0.01 inch, the agreement between calculated and experimental results for this test condition may be within 5 percent. In general, the average of the experimental data for the left wing, with optimum interpretation of the precision, is less than 5 percent from the calculated values.

Examination of the time histories on figures 13(a) and 14(a) shows that the actual oscillations of the wing, subsequent to peak wing-tip deflection, are not checked by the calculated results. This difference is caused by the necessity of choosing a constant division of damping coefficient in the equivalent system to represent a given gust condition. The method of application and the

amount of vibratory damping, however, appears satisfactory when compared in figure 12 with the results obtained when all vibratory damping is omitted from the calculations.

The results of the comparison of experimental and calculated data for the flexible wing model then indicate that the method of calculation is adequate for prediction of the ratio of maximum dynamic wing-tip deflections to maximum fuselage acceleration on encountering certain single gust shapes.

Limitations of Calculations

Limitations shown by model tests.- The applicability of the forcing function Ate^{-bt} is best shown by the comparisons of the calculated and experimental time histories of acceleration increment for the model in the rigid condition (fig. 15). Since the comparisons shown were made by adjusting the calculated curves so that the maximum values of acceleration increment agreed with the experimental results, any discussion must be based on the shapes of the curves alone. It is thought that the greatest part of the discrepancies between the curves in figure 15 may be ascribed to the effects of pitching motion. The form of the forcing function for each gust gradient is intended to include the amount of pitching motion indicated by the band of data of $\frac{\Delta\theta/57.3}{U/V}$ shown in figure 11. The $\frac{\Delta\theta/57.3}{U/V}$ ratios for the rigid-wing condition of the model do not all fall within this band of data. The direction in which these ratios differ would tend to explain the difference between the experimental and calculated curves of figure 15, except for the long gradient-distance case (fig. 15(c)) where the experimental and calculated curves appear to agree perfectly, although the $\frac{\Delta\theta/57.3}{U/V}$ ratio for this case is the furthest from that expected (fig. 11). If, however, the experimental values of acceleration increments were raised to consider the pitch correction and the calculated values were increased in proportion to the new maximum acceleration increment, the two curves would again closely coincide. It would appear then that the forcing function in the form of Ate^{-bt} is adequate for calculation purposes; however, care should be exercised in its application to be sure that in a gust the stability of the airplane intended for calculation approximates that indicated by the band of data in figure 11. If not, recourse should be made to alternative methods of calculation mentioned previously.

The comparison in figure 11 of the $\frac{\Delta\theta/57.3}{U/V}$ ratios for the flexible conditions of the test model with those for the rigid conditions indicates that the assumption of the same pitching stability for both rigid and flexible conditions is in error. It appears therefore that an investigation should be made to determine the importance of the effect of wing flexibility on the stability of an airplane in a gust.

Whereas the effect of a constant division of damping coefficient appears to be negligible when the present method is used to predict the maximum responses to single gusts, the obvious overdamping of the vibratory wing motion subsequent to maximum wing-tip deflection might well lead to an error, if the results for single gusts were superimposed in order to obtain results for a succession of gusts. Considerable care should be exercised, therefore, when interpreting results for repeat gusts that are determined from single-gust results based on the calculation method of this paper.

In general, the limitations of the method of calculation brought out by comparison with results of model tests are thought not to affect seriously the results calculated for the response to single gusts. A certain amount of dispersion from the pitching stability assumed by the forcing function Ate^{-bt} does not appear to affect seriously the results when presented in ratio form. It is apparent that, when the results for single gusts are superimposed to obtain results for successive gusts, the calculations for the single gusts must be made with greater attention to factors such as the shape of the forcing function and the effect of the assumption of a constant division of damping load.

Other limitations.- Other limitations of the method of calculation are apparent in the assumptions that only the fundamental mode of wing bending is excited and that the gust is uniform along the span of the airplane. When the actual spanwise distributions of gust velocity shown in reference 5 are considered, it is apparent that the response in modes other than the fundamental mode of bending and the effect of roll and yaw of the airplane should be investigated.

Although, for further simplification, wing torsion was neglected in the present analysis, twisting of the wing under dynamic conditions in combination with wing bending may readily have an adverse effect on the loads for which an airplane must be designed.

The method of analysis presented in this paper should either be extended or replaced by another method so that wing torsion, other modes of bending, and the effects of unsymmetrical gusts are considered.

Results Calculated for Effect of Change of Certain Parameters

General results.- The results of the calculations given in figure 16 for all the airplanes chosen show that the dynamic-stress ratio in all cases increases from an understress for a gust of long gradient distance to moderate or high overstress for a gust of short gradient distance. The general shape of the curves seems to indicate that even higher overstress would occur in sharper gusts than those gusts examined. The lag in the development of lift in the gusts of short gradient distance would preclude, however, such a result, since even for an infinitely sharp gust, the forcing function would be similar to that for a gust with a gradient distance of about 4 chords. Note that, although the dynamic-stress ratios appear to approach zero as the gradient distance of the gust increases, this condition is not the actual case but results from the fact that, when the calculations were made, account was not taken, in the division of the damping coefficient, of the changing relative significance of the vibration and of the over-all vertical velocities of the wing. If the correct division had been made for the gusts with a gradient distance of 20 chords, the dynamic-stress ratio would tend to approach 1.0 for most of the cases shown in figure 16.

The results of the calculations shown in figure 16 for models A, C, and D show that, at the design gust of gradient distance of 10 chords, which is assumed for most conventional airplanes, the dynamic-stress ratio varies from about 8-percent understress to about 12-percent overstress. Although at this time a designer cannot take advantage of small amounts of understress, when overstress is indicated by the calculations, it is thought that this indication should be considered in the design of the airplane.

Although, for the airplanes considered, the fuselage acceleration ratio does not appear to vary much from a value of 1, the wing-tip acceleration ratio at 10 chords is as high as 2.7 in one case and greater than 1.6 in most of the cases. This variation indicates that the wing-tip acceleration ratio should be examined when concentrated masses or wing components near the wing tip are considered in a design.

Effect of a change of wing frequency caused by a change in wing stiffness.- The calculations made for the gust-tunnel tests discussed previously show the effect on the dynamic-stress ratios of a change of stiffness of a wing such as to halve approximately the frequency of vibration of the wing. Examination of figure 17, which gives a comparison of the dynamic-stress ratios for the two conditions, shows that at present nothing can be concluded from the results because, although the ratio for the higher wing-frequency case is the higher in the shortest gradient gust, the ratio becomes lower than the low-frequency case as the gradient increases. At the critical gradient distance of 10 chords, the high-frequency case shows, however, a reduction in dynamic-stress ratio of 14 percent below the low-frequency case. Further analysis of this particular question is therefore needed before the conclusion can be reached that a reduction of wing frequency in this manner tends to increase the dynamic-stress ratio at the critical gradient distance.

Effect of simplification by omitting parts of the damping.- The comparison of the dynamic-stress ratios for the two calculation conditions for model B (fig. 18) and the effect (fig. 12) of eliminating vibratory damping from the calculations serve to illustrate that simplification of the method by omitting parts of the damping does not appear feasible.

Effect of a change in forward velocity of an airplane.- The results given in figure 19 illustrate the change brought about in the three ratios by increasing the forward velocity of model C from 200 to 400 miles per hour. The increase of velocity together with the corresponding increase in the rate of application of the gust load would appear to result in an increase in the dynamic-stress ratio. Figure 19, however, shows that the ratio does not vary much as the speed increases and this lack of variation is thought to be caused partly by the fact that the aerodynamic damping increases directly as the speed and tends to offset the expected increase in dynamic stress. While the results for the fuselage acceleration ratio show a similar trend, the wing-tip acceleration ratio increases from about 1.8 to 2.5 as the speed is doubled, which further emphasizes the recommendation that the wing-tip acceleration ratio be considered when concentrated masses or wing components near the wing tip are considered in a design.

Effect of a change of wing frequency caused by a change in flight-weight condition.- The calculations for model D were made to show the effect on the dynamic-stress ratios of a change in flight condition from normal gross weight to overload gross weight. Table II shows that the forward velocity is different in the two cases, but consideration of the foregoing discussion may justify

the assumption that this factor is negligible. The results are given in figure 20, with dynamic-stress ratio plotted as a function of the gradient distance of the gust. A reduction in wing frequency brought about by the addition of mass is shown to result in an increase in the dynamic-stress ratio. Further analysis and calculations appear to be needed, but a tentative conclusion is made that for a conventional airplane a reduction in wing frequency caused by the addition of mass results in an increase in the dynamic-stress ratio.

Effect of repeated gusts on the dynamic-stress ratios.- The results of calculations for models C and D were presented previously in reference 11, and the values of table IV are taken from table II of that paper and show the most serious values of overstress for two gusts from a combination of the calculations for a single gust. Table IV shows that no definite correlation exists between the effect of gradient distance of the first and second gusts and the distance between them H_3. This lack of correlation results from the influence of certain other factors, such as the relation between the time to peak acceleration and the period of wing vibration, which complicate the problem when the reactions to one gust are superposed on the reactions to another gust.

Examination of the values in table IV shows that substantial overstress exists for all the combinations of gusts presented and that the addition of a short gradient gust produces the largest value of overstress. As indicated previously, however, the gust velocity measured by an airplane tends to decrease from a maximum for a gradient distance of 10 chords as the gradient distance is decreased. As a result, the values of dynamic stress to be considered are those (indicated by the footnote in table IV) that represent the combination of the reactions to gusts having a gradient distance of 10 chords. Before an estimate can be made as to whether the overstress shown for the airplanes in question is serious, it is necessary to consider the conditions upon which the values in table IV were calculated and the effect of the intensity and size of gusts and their spatial distribution in the atmosphere.

The results shown in table IV were based simply on the premise that the quantity of interest was the ratio of maximum stress obtained under dynamic conditions to the maximum stress that would be computed under static conditions without regard to velocity or spacing of such pairs of gusts in the atmosphere. Examination of the time histories of reactions given in figures 24 to 26 indicates that for each case shown the dynamic-stress ratio given in table IV is the ratio of the maximum dynamic deflection in the second gust

to the static deflection δ_{st} computed from the maximum value of Δn_r in the second gust. As pointed out in reference 11, however, when design conditions are considered, the ratio to use is that of the maximum dynamic deflection of the whole sequence to the deflection computed from the static load in the first gust because, if the two gusts were each of design velocity, the design static load would be attained on passage through the first gust. The values determined on this basis for the succession of two gusts of 10-chord gradient distance indicated in the table would then be as follows:

Model	Condition	δ_d/δ_{st}
C	1	1.62
D	1	1.58
D	2	1.64

An analysis given in reference 11, however, based on frequency data of single gusts, indicated that the gust velocities of two repeated gusts would range from 0.61 to 0.75 the velocity of the single design gust so that, multiplied by these ratios, the dynamic-stress ratios given would be reduced to an average of 1.10 times the design stress.

A recent statistical analysis of the characteristics of repeated gusts in turbulent air (reference 12) provides more concrete data, however, than the analysis used in reference 11. Two conclusions from reference 12 state that sets of two repeated gusts with average absolute effective gust velocities of 25 feet per second apparently are encountered in turbulent air as often as single gusts of intensity greater than 30 feet per second, and that the over-all average spacing between two repeated gusts is about 25 chords. Note that spacing as defined in the reference paper is the distance between acceleration peaks and in the terminology of this paper would correspond to the sum $H_2 + H_3$.

Table IV shows that the sums of $H_2 + H_3$ in the cases indicated by the footnote do not approximate 25 chords; therefore, a new superposition of the responses to single gusts of 10 chords was made so that the spacing would be 25 chords. The dynamic-stress ratios for the three cases were then determined as the ratios of the maximum dynamic deflection in the sequence to the deflection computed from the static load imposed by the first gust and the results were reduced by the ratio of the average gust

velocity for two repeated gusts to the design velocity for a single gust which is 25/30. The results determined on this basis are compared with the results for the single gusts of 10 chords in the following table:

Model	Condition	Design repeated gusts $\delta_{d_{max}}/\delta_{st}$	Design single gusts $\delta_{d_{max}}/\delta_{st}$
C	1	0.96	1.07
D	1	1.08	0.92
D	2	1.10	1.09

The variation in the results indicates that the dynamic-stress ratios for a design repeat gust should be investigated. The results also indicate, however, that these dynamic-stress ratios are not likely to be much greater than those which would be determined for a design single gust.

CONCLUSIONS

Analytical Method and Experimental Work

It appears from consideration of the comparison of the experimental work and associated calculations that:

1. The analytical method as presented in this paper is of sufficient accuracy to predict the ratio of the maximum dynamic wing-tip deflection increment to the maximum fuselage acceleration increment for a conventional airplane.

2. Simplification of the method by omitting parts of the damping does not appear feasible.

Calculations

The analysis of the results of the calculations for the effect of change of certain gust and airplane parameters indicates:

1. The dynamic-stress ratio for airplane wings from encountering gusts increases as gradient distance decreases.

2. For the assumed design gust with the gradient distance of 10 chords, the overstress in a single gust may be as much as 12 percent.

3. Although the results for the two airplanes each of which encountered one type of repeated gust were not considered conclusive, a repeated gust does not seem to be more critical than a single gust.

4. For the assumed design gust of 10-chord gradient distance, the wing-tip acceleration increment is generally much greater than the fuselage acceleration increment and should be taken into account when designing for concentrated masses or wing components near the wing tip.

5. For the assumed design gust of 10-chord gradient distance the dynamic-stress ratio does not change appreciably with change in forward velocity of the airplane, but an increase in speed is accompanied by an increase in the wing-tip acceleration ratio.

6. A reduction in wing frequency either by a change in stiffness or by a change in weight increases the dynamic-stress ratio at the assumed design gust of 10-chord gradient distance.

Langley Memorial Aeronautical Laboratory
National Advisory Committee for Aeronautics
Langley Field, Va., January 15, 1947

APPENDIX

DETAILS OF METHOD AND PROCEDURE FOR DETERMINATION OF CONSTANTS

Certain assumptions were made to simplify the problem of determining the dynamic response of airplane wings on encountering gusts. These assumptions are:

(1) The imposed gust loads are symmetrical about the center line of the airplane and their characteristics in the line of flight are known.

(2) The imposed gust loads excite only the fundamental mode of bending of the wing with the result that the stress in the wing is proportional to the deflection of the wing tip.

(3) The forward velocity of the airplane is constant during passage through the gust.

Together with these assumptions, an airplane is reduced to the equivalent biplane shown in figure 1. The equations of motion of the two parts of the equivalent biplane are reduced to linear equations with constant coefficients. The solution of the equations and the method of determination of coefficients follow.

Solutions of Equations

General equations.- The equations for which the solutions follow contain the type of forcing function used for calculations in this paper.

$$M_{w_e} \frac{d^2\delta_w}{dt^2} + \lambda_{w_e} \frac{d\delta_w}{dt} + K(\delta_w - \delta_f) = A_{w_e} te^{-bt} \tag{A1}$$

$$M_{f_e} \frac{d^2\delta_f}{dt^2} + \lambda_{f_e} \frac{d\delta_f}{dt} - K(\delta_w - \delta_f) = A_{f_e} te^{-bt} \tag{A2}$$

Since equations (A1) and (A2) are simultaneous linear differential equations, equation (A2) may be solved for δ_w and the result substituted for δ_w in equation (A1). This process leads to the following:

$$\left(D^4 + a_1D^3 + a_2D^3 + a_3D\right)\delta_f = F_1te^{-bt} + F_2e^{-bt} \tag{A3}$$

where

$$a_1 = \frac{\lambda_{w_e}M_{f_e} + \lambda_{f_e}M_{w_e}}{M_{w_e}M_{f_e}} \tag{A4a}$$

$$a_2 = \frac{K\left(M_{w_e} + M_{f_e}\right) + \lambda_{w_e}\lambda_{f_e}}{M_{w_e}M_{f_e}} \tag{A4b}$$

$$a_3 = \frac{K\left(\lambda_{w_e} + \lambda_{f_e}\right)}{M_{w_e}M_{f_e}} \tag{A4c}$$

$$F_1 = \frac{A_{w_e}K}{M_{w_e}M_{f_e}} + \frac{A_{f_e}}{M_{f_e}}\left(b^2 - \frac{\lambda_{w_e}b}{M_{w_e}} + \frac{K}{M_{w_e}}\right) \tag{A5a}$$

$$F_2 = \frac{A_{f_e}}{M_{f_e}}\left(\frac{\lambda_{w_e}}{M_{w_e}} - 2b\right) \tag{A5b}$$

Equation (A3) may be recognized as a linear differential equation with constant coefficients which may be solved by methods commonly used for solving differential equations. Solution for δ_f is

$$\delta_f = c_1 e^{-R_1 t} (\cos R_2 t) + c_2 e^{-R_1 t} (\sin R_2 t) + c_3 e^{-R_3 t}$$

$$+ c_4 + \frac{F_1}{G_1} t e^{-bt} + \left(\frac{F_2}{G_1} + \frac{F_1 G_2}{G_1} \right) e^{-bt} \tag{A6}$$

where R_1 and R_2 are the real and imaginary parts of the complex roots $R_1 \pm R_2\sqrt{-1}$ and R_3 is the real root of the cubic equation derived from equation (A3); c_1, c_2, c_3, and c_4 are constants of integration; and in the particular integral of the solution:

$$G_1 = b^4 - a_1 b^3 + a_2 b^2 - a_3 b \tag{A7a}$$

$$G_2 = 4b^3 - 3a_1 b^2 + 2a_2 b - a_3 \tag{A7b}$$

In the case where $G_1 = 0$ a special solution of the equation would be required, but this solution can be obviated by choosing a slightly different value for b.

Equation (A2) is solved for the deflection of the equivalent wing with respect to the equivalent wing-fuselage $(\delta_w - \delta_f)$ and for the space position of the equivalent wing δ_w. The resulting equations follow:

$$\delta_w - \delta_f = \frac{M_{f_e}}{K} \frac{d^2\delta_f}{dt^2} + \frac{\lambda_{f_e}}{K} \frac{d\delta_f}{dt} - \frac{A_{f_e} t e^{-bt}}{K} \tag{A8}$$

$$\delta_w = \frac{M_{f_e}}{K} \frac{d^2\delta_f}{dt^2} + \frac{\lambda_{f_e}}{K} \frac{d\delta_f}{dt} + \delta_f - \frac{A_{f_e} t e^{-bt}}{K} \tag{A9}$$

The vertical velocities of the equivalent wing-fuselage and of the equivalent wing are determined from the first derivatives of equations (A6) and (A9), respectively, and the normal accelerations are determined from the second derivatives.

In order to perform an arithmetical solution for a particular airplane, it has been found advisable to insert the pertinent numerical constants for the airplane in equation (A3) and solve. In addition, experience has shown it necessary to carry eight to ten significant figures throughout the solution so that the results are useful because, at different stages in the evaluation, small differences of large quantities are obtained.

Rigid-wing acceleration increment.- The normal gust-load design procedure assumes that the load is applied statically and that the normal acceleration is constant along the span of the airplane. The difference between this assumption and the actual case is shown by ratios of the accelerations determined under dynamic conditions to the accelerations that would be determined if the airplane were rigid. In order that the comparison be valid, the rigid airplane acceleration increment Δn_r is determined as the response of the equivalent biplane to the over-all forcing function on the airplane when the springs are replaced by rigid rods. With this restriction equations (A1) and (A2) may be combined to become

$$\Delta n_r + \lambda_c \int_0^t \Delta n_r \, dt = A_c t e^{-bt} \qquad \text{(A10)}$$

where

$$\Delta n_r = \frac{d^2\delta_w}{dt^2} = \frac{d^2\delta_f}{dt^2}$$

and

$$\lambda_c = \frac{\lambda_{w_e} + \lambda_{f_e}}{M_{w_e} + M_{f_e}}$$

$$A_c = \frac{A_{w_e} + A_{f_e}}{M_{w_e} + M_{f_e}}$$

When the integral in equation (A10) is removed by differentiation, the equation becomes a linear differential equation with constant coefficients which may be solved in the same manner as equation (A3). The complete solution is:

$$\Delta n_r = \left[\frac{A_c}{\lambda_c - b} + \frac{A_c b}{(\lambda_c - b)^2}\right]\left(e^{-bt} - e^{-\lambda_c t}\right) - \frac{A_c b}{c - b} te^{-bt} \qquad (A11)$$

Static deflection and dynamic-stress ratio.- The static deflection used in the dynamic-stress ratio to represent the static stress in the wing is considered as the deflection of the upper wing of the equivalent biplane under the conditions of the normal static design procedure. The static deflection is then computed as follows:

$$\delta_{st} = \frac{\Delta n_{r_{max}}\left(L_1 W - W_{w_e}\right)}{K} \qquad (A12)$$

The ratio of the maximum value of dynamic wing-tip deflection $\delta_{d_{max}}$, as determined by equation (A8), to the static deflection δ_{st} is called the dynamic-stress ratio since the stress, determined under static conditions, is multiplied by this ratio to take into account dynamic conditions.

Determination of Constants for the Equations

Required conditions.- In determining the values of the coefficients for the equivalent biplane, the following conditions should be satisfied:

(1) The total mass and the total load on the equivalent biplane should be identical with those of the original airplane.

(2) The kinetic energy of vibration of the upper wing should closely approximate that of the original wing beam for an amplitude of vibration of the upper wing equal to that of the tip of the original wing.

(3) The natural frequency should be the same as that for the fundamental mode of the original wing.

(4) The upper wing should deflect under the equivalent static load the same amount that the wing tip of the airplane does under the corresponding aerodynamic static-load distribution.

(5) The damping coefficient of the upper wing should represent, at least to peak load, the damping of the motion of the wing.

Equivalent masses M_{w_e} and M_{f_e}.- The equivalent mass M_{w_e} is obtained from an approximate requirement that the kinetic energy of vibration of the original wing beam is reproduced by the upper wing of the equivalent biplane. The equivalent mass of the fuselage M_{f_e} is taken equal to the total mass of the airplane minus M_{w_e}.

In the absence of more definite information the combined effect of concentrated masses and nonuniform wing structure is assumed to be such that the equivalent wing mass may be determined from the following relation which represents an approximation to that which would be derived for a uniform cantilever beam. Thus,

$$M_{w_e} = 2\sum_{0}^{\bar{x}}\left[\Delta M\left(\frac{x}{\bar{x}}\right)^3\right]$$

(see fig. 1) where $\bar{x}$ is the distance from wing root to tip and x is the distance to the individual mass ΔM. For special cases, such as strut-supported wings and arrangements other than the conventional cantilever monoplane, other suitable approximations can be devised. If the wing were a uniform cantilever beam, M_{w_e} would be approximately 24 percent of the mass of the wing (reference 13, pp. 83-89).

Equivalent spring constant K.- The equivalent spring constant defines the springs in the equivalent biplane which allow approximately the same frequency as the cantilever wing of the original airplane. The value of K may be approximated by using M_{w_e} and the known or estimated wing frequency in the relation:

$$f = \frac{1}{2\pi}\sqrt{\frac{K}{M_{w_e}}}$$

Air loads or forcing functions.- As in the case of the mass of the airplane, the total air load must be divided into the components affecting the motions of the fuselage and wing tip of the original airplane. If the deflection of the wing tip under a given static air load is known, the transfer to the equivalent biplane is accomplished by merely determining the load applied to the equivalent spring which gives that same deflection to the upper wing of the equivalent biplane. The remainder of the load is then applied to the lower wing-fuselage combination. Any air load of the same type as this static air load may be divided into the same proportion and applied to the equivalent system to give the same deflections and reactions as the load causes on the original airplane.

Data on deflection, however, is often not available. Recourse may then be made to several methods of determining the division of loads. One simple approximation is to assume that the wing of the airplane is a uniformly stiff cantilever from root to tip. Then, if the beam is considered to be weightless, the equation for the deflection of the tip of the beam under a concentrated load placed at the tip is compared with the equations of deflection for two types of loading distributed along the beam as follows: a uniform load along the beam and a load uniformly tapering from a maximum at the root to zero at the tip. The differences in the three equations are in the numerical "efficiency" factors which are one-third for the concentrated load, one-eighth for the uniform load, and one-fifteenth for the tapered load. A concentrated load at the tip of a cantilever beam that will give the same deflection as a uniform load is then one-eighth divided by one-third or three-eighths of the uniform load, and the equivalent concentrated load to replace the tapered load is three-fifteenths of the tapered load. The estimate of the shape of the span loading of a given airplane probably falls somewhere between that of a uniform load and of a tapered load so that a comparison of these shapes indicates that between 20 and 37.5 percent of the total load produces the tip deflection and the remainder is considered as acting at the wing root. If the wing under consideration does not approximate closely enough a uniform cantilever, allowance for this discrepancy can be made in choosing the percentages of load.

The forcing functions $A_{w_e} te^{-bt}$ and $A_{f_e} te^{-bt}$ in equations (A1) and (A2) represent the air load on the wing apart from the damping, divided as in the previous discussion, where

$$A_{w_e} + A_{f_e} = A$$

and

$$A = \frac{\Delta n_a W}{te^{-bt}} \quad \text{at} \quad bt = 1 \quad \text{or} \quad Wbe\Delta n_a \tag{A13}$$

Δn_a arbitrary load factor increment the airplane would experience if it had no vertical motion when traversing the gust

$b = \frac{1}{t}$ at $bt = 1$ or at the maximum value of the function te^{-bt}

The next problem is the determination of a value of b so that the forcing function represents a gust of a given shape. Gust-tunnel tests of relatively stable and rigid models (reference 6) have shown that the peak of the acceleration-increment curve occurs at the end of H_1, as given in figure 2(a). The time necessary to reach the maximum value of the time history curve of the rigid-wing acceleration increment, which is obtained from the forcing function curve by use of equation (A11), is assumed, therefore, to represent the length of the gradient of the gust imposed on the airplane. Since the peaks of the forcing-function curve and the acceleration-increment curve do not occur at the same time except in the case of an airplane of infinite mass, the following procedure for the determination of a value for b has been derived.

(1) Three or four values of b are chosen so that they represent a range of peak values of the forcing function corresponding to from 2 chords of travel of the airplane to 40 or 50 chords of travel.

(2) The time necessary to reach the maximum value of Δn_r is determined for each value of b chosen and converted to chords of travel of the airplane.

(3) A plot is made of b against chords of travel to peak of the Δn_r curve.

(4) The values of gust gradient distance chosen for the calculations are then used with the curve plotted in step 3 to determine the corresponding values of b.

If the forcing function Ate^{-bt} does not adequately represent the case considered, the actual forcing function for the sharp-edge gust may be determined from calculations similar to those calculations outlined in reference 7 or by recourse to gust-tunnel tests.

Equations (A1) and (A2) would then be solved for a unit-function type of forcing function (reference 8) and the result built up into the response of the flexible airplane to a sharp-edge gust by the graphical method outlined in reference 9. This response of the flexible airplane to a sharp-edge gust may then be considered as the response to a unit-function-type gust and be again built up to represent the response of the flexible airplane to any type of symmetrical gust.

Damping factor λ.- Consideration of the reaction of an airplane to a given gust or the reaction of the equivalent biplane to the forcing function indicates that two distinct motions have to be damped - the vertical motion of the airplane as a whole and the vibratory motion of the wing itself. Since the vertical motion rises from the action of unsteady lift, the damping of this motion is also subject to unsteady lift effects. The vibratory motion of the wing falls in this category because the lift of an oscillating airfoil has been shown (references 14 and 15) to be affected by unsteady lift phenomena. Determination of the effects of this unsteady lift is therefore necessary in order to predict correctly the dynamic stress of an airplane wing upon entry into a gust. The obvious solution would be to include the equations of unsteady-lift damping directly in the dynamic-stress equations, but this procedure would destroy the linearity of the equations and make them very difficult to solve. The steady-lift damping would be $\frac{\rho}{2} mSV$ times the velocity of oscillation with $\frac{\rho}{2} mSV$ a constant for a given case. Inasmuch as having the damping coefficient in this form would fulfill the conditions for normal solution of the original equations, an analysis and some tests were made to determine whether the effect of unsteady lift on the damping force could be considered to reduce the steady-lift damping force by a constant factor - a damping-efficiency factor - without seriously impairing the results.

The analytical determination of this factor was derived from the following expression for the change in C_L brought about by a sudden change in angle of attack:

$$\Delta C_L = m \int_0^{s_1'} C_{L_\alpha} (s_1' - s') \frac{d\alpha}{ds'} ds' \qquad (A14)$$

where

ΔC_L change in coefficient of lift

m slope of lift curve, radians

C_{L_α} ratio of absolute value of the unsteady-lift function for a sudden change in angle of attack to its absolute value at $t = \infty$ for a wing of aspect ratio of 6

s_1' distance of travel from initiation of angle-of-attack change to point at which lift is desired, half chords

s' distance of travel from initiation of angle-of-attack change, half chords

$\frac{d\alpha}{ds'}$ rate of change of angle of attack with half chord of travel

Substitution of Jones' approximation of the unsteady-lift function for aspect ratio 6 for a sudden change in angle of attack (reference 16, equation (29)) changed to ratio form

$$C_{L_\alpha}(s_1' - s') = 1.000 - 0.361e^{-0.381(s_1'-s')}$$

is made in equation (A14). Then, assuming a simple harmonic vertical motion of the wing, the following substitution is made:

$$\frac{d\alpha}{ds'} = \frac{Xk}{V} \sin ks'$$

where

$\alpha = \frac{U}{V}$

U vertical velocity of wing

V horizontal velocity of wing

X measure of the maximum vertical velocity of wing

$k = \frac{2\pi}{s_o'}$

and

s_o' distance of travel of wing for one period of oscillation, half chords

The indicated integration in equation (A14) is performed and the result is divided by the assumed steady-lift damping such that the damping-efficiency factor is given by

$$\frac{-C_1 \cos ks_1' - C_2 \sin ks_1' + 1.000 + C_3 e^{-0.381 s_1'}}{1 - \cos ks_1'} \qquad (A15)$$

where

$$C_1 = 1.000 - \frac{0.361k^2}{0.145 + k^2}$$

$$C_2 = -\frac{0.138k}{0.145 + k^2}$$

$$C_3 = -\frac{0.361k^2}{0.145 + k^2}$$

Evaluation of expression (A15) for a series of ratios of wing frequency to half chords of travel shows that the damping-efficiency factor varies considerably throughout a cycle of oscillation of the wing, but the greatest variation occurs as the vibration velocity approaches zero or at the point of minimum damping force. As a result, an average value of 75 percent for the magnitude of the damping-efficiency factor was taken from the parts of the cycle where the damping force was near the maximum value so that the total damping coefficient λ is given by the equation:

$$\lambda = 0.75 \frac{\rho}{2} mSV$$

In order to obtain an experimental verification of the method and result of the theoretical determination of damping-efficiency factor, tests were conducted on a 10-inch half-span half-model at three different wind speeds in the $\frac{1}{15}$-scale model of the full-scale tunnel. Oscillatory motion about a flexure plate hinge at the wing root was begun by the decrease in lift caused by the sudden deflection to zero of a plain flap that formed the entire trailing edge of the wing. The flap motion and the wing-tip motion were recorded as time histories and the damping coefficients were then determined from the logarithmic decrements of the wing-tip oscillations (reference 13, p. 35). The results of these tests indicated that the value of 75 percent determined by the theoretical analysis was a valid quantity for the damping-efficiency factor.

The damping coefficients for the upper wing and lower wing-fuselage must now be determined. The proper values for the individual coefficients are dependent upon the spanwise distribution of the vertical velocities of the original wing which changes as the airplane penetrates the gust. In the case of uniform spanwise distribution of vertical velocity (case 1), the airplane damping coefficient λ is divided in the same way as the impressed air-load coefficient so that

$$\lambda_{w_e} = \frac{1}{4}\lambda$$

$$\lambda_{f_e} = \frac{3}{4}\lambda$$

For the case where the spanwise distribution of vertical velocity equals the deflection curve of the assumed uniform cantilever wing of the original airplane (case 2), the total damping load on the original wing is concentrated near the wing tip and is approximately equal to λ times one-third the tip velocity. When this situation is applied to the equivalent biplane, the total damping on the equivalent biplane is applied to the upper wing so that λ_{w_e} is then equal to $\frac{1}{3}\lambda$.

Case 2 represents the situation as the airplane first penetrates the gust and case 1 represents the situation later in the penetration when the vibration has damped out. In order to avoid destroying the linearity of equations (A1) and (A2), coefficients chosen on the basis of conditions existing at maximum load are used to calculate the entire time history. If case 1 exists, the time

histories of reactions calculated are not seriously affected; however, when case 2 exists, the time histories subsequent to peak load would be quite seriously in error. In order to account for this inaccuracy and to effect a transition between the two cases, λ_{f_e} is taken equal to $\frac{2}{3}\lambda$ in case 2. This assumption will not affect the results for the penetration into the gust represented by case 2, because the vertical velocity of the fuselage of the original airplane and the wing-fuselage of the equivalent biplane would be zero.

In order to provide a way to determine which division of damping coefficient is applicable in a given calculation, an arbitrary criterion was found that depended on the relation between the airplane vertical velocity, which was determined by integrating the time history of the rigid-wing acceleration increment Δn_r to its maximum value, and the vibration velocity of the wing, as determined by dividing the static deflection δ_{st} by the time required to reach maximum Δn_r from the beginning of the gust. When the ratio of airplane vertical velocity to the vibration velocity is less than 5, the division into one-third and two-thirds applies, and when the ratio is greater than 5, the damping coefficient is divided into one-fourth and three-fourths. Note that the divisions of damping coefficient given apply in particular to conventional cantilever-wing airplanes. Other types of airplanes would require special analysis.

REFERENCES

1. Küssner, Hans Georg: Stresses Produced in Airplane Wings by Gusts. NACA TM No. 654, 1932.

2. Bryant, L. W., and Jones, I. M. W.: Stressing of Aeroplane Wings due to Symmetrical Gusts. R. & M. No. 1690, British A.R.C., 1936.

3. Williams, D., and Hanson, J.: Gust Loads on Tails and Wings. R. & M. No. 1823, British A.R.C., 1937.

4. Sears, William R., and Sparks, Brian O.: On the Reaction of an Elastic Wing to Vertical Gusts. Jour. Aero. Sci., vol. 9, no. 2, Dec. 1941, pp. 64-67.

5. Moskovitz, A. I.: XC-35 Gust Research Project - Preliminary Analysis of the Lateral Distribution of Gust Velocity along the Span of an Airplane. NACA RB, March 1943.

6. Donely, Philip: An Experimental Investigation of the Normal Acceleration of an Airplane Model in a Gust. NACA TN No. 706, 1939.

7. Donely, Philip, Pierce, Harold B., and Pepoon, Philip W.: Measurements and Analysis of the Motion of a Canard Airplane Model in Gusts. NACA TN No. 758, 1940.

8. Berg, Ernst Julius: Heaviside's Operational Calculus. McGraw-Hill Book Co., Inc., 1936.

9. Jones, Robert T.: Calculation of the Motion of an Airplane under the Influence of Irregular Disturbances. Jour. Aero. Sci., vol. 3, no. 12, Oct. 1936, pp. 419-425.

10. Rhode, Richard V.: Gust Loads on Airplanes. SAE Jour., vol. 40, no. 3, March 1937, pp. 81-88.

11. Pierce, Harold B.: Dynamic Stress Calculations for Two Airplanes in Various Gusts. NACA ARR, Sept. 1941.

12. Moskovitz, A. I., and Peiser, A. M.: Statistical Analysis of the Characteristics of Repeated Gusts in Turbulent Air. NACA ARR No. L5H30, 1945.

13. Timoshenko, S.: Vibration Problems in Engineering. Second ed., D. Van Nostrand Co., Inc., 1937.

14. Küssner, H. G.: Zusammenfassender Bericht über den instationären Auftrieb von Flügeln. Luftfahrtforschung, Bd. 13, Nr. 12, Dec. 20, 1936, pp. 410-424.

15. Theodorsen, Theodore: General Theory of Aerodynamic Instability and the Mechanism of Flutter. NACA Rep. No. 496, 1935.

16. Jones, Robert T.: The Unsteady Lift of a Wing of Finite Aspect Ratio. NACA Rep. No. 681, 1940.

TABLE I

CHARACTERISTICS OF THE TEST MODEL AND EQUIVALENT CONSTANTS FOR CALCULATION

Values constant for tests			
Weight, lb	1.832	Pitching moment of inertia, slug-ft^2	0.00782
Wing area, sq ft	1.183	Radius of gyration of wing, ft	0.663
Mean geometric chord, ft	0.394	Weight of wing, lb	0.293
Span, ft	3.0	Mass ratio, M_{w_e}/M	0.0333
Slope of lift curve, per radian	4.73	Air load ratio, A_{w_e}/M	0.37
Forward velocity, fps	61.0	Damping factor, λ, lb-sec/ft	0.2954
Gust velocity, fps	6.0		

Values changed in tests						
Variables	f = 13.5 cps; K = 13.608 lb/ft			f = 26.1 cps; K = 51.024 lb/ft		
	Gust 1	Gust 2	Gust 3	Gust 1	Gust 2	Gust 3
Gradient distances of gust, chords	4.6	7.8	21.2	4.6	8.8	22.4
Damping ratio, λ_{w_e}/λ	0.50	0.50	0.37	0.50	0.50	0.37
Forcing-function factor, A, lb/sec	275.948	151.921	37.2580	275.948	132.495	38.7523
Time constant, b, per sec	27.70	15.25	3.74	27.70	13.30	3.89

NATIONAL ADVISORY
COMMITTEE FOR AERONAUTICS

TABLE II

CHARACTERISTICS OF AIRPLANES CHOSEN FOR CALCULATIONS

Airplane	Condition	Weight (lb)	Wing area (sq ft)	Wing loading (lb/sq ft)	Span (ft)	Mean geometric chord (ft)	Natural wing frequency (cps)	Slope of lift curve (per radian)	Number of engines	Forward velocity (mph)	Remarks
Model A	1	100,000	1700	58.8	113.8	14.93	2.20	4.73	4	256	Hypothetical airplane scaled from flexible wing model
	2	100,000	1700	58.8	113.8	14.93	4.25	4.73	4	256	
Model B	1	44,860	2480	18.1	150.0	18.53	3.89	4.76	4	200	Fuselage damping omitted in condition 2
	2	44,860	2480	18.1	150.0	18.53	3.89	4.76	4	200	
Model C	1	100,000	1710	58.5	140.0	12.21	2.45	5.04	4	260	Speeds assumed for calculation
	2	100,000	1710	58.5	140.0	12.21	2.45	5.04	4	200	
	3	100,000	1710	58.5	140.0	12.21	2.45	5.04	4	300	
	4	100,000	1710	58.5	140.0	12.21	2.45	5.04	4	400	
Model D	1	62,500	1826	34.2	140.0	13.04	2.50	4.93	2	190	Normal gross weight
	2	102,000	1826	56.0	140.0	13.04	1.43	4.93	2	160	Overload gross weight

NATIONAL ADVISORY
COMMITTEE FOR AERONAUTICS

TABLE III

CHARACTERISTICS AND CALCULATION DATA FOR BIPLANE EQUIVALENTS OF AIRPLANES IN TABLE II

Biplane equivalent of	Condition	Gradient distance, H_1 (chords)	Weight (lb)	M_{w_e} (slugs)	$\frac{M_{w_e}}{M}$	Damping factor, λ (lb-sec/ft)	$\frac{\lambda_{w_e}}{\lambda}$	Forcing function factor, A (lb/sec)	$\frac{A_{w_e}}{A}$	Spring constant, K (lb/ft)	Time constant, b (per sec)
Model A	1	4.6 9.0 22.0	100,000	103.33	0.0333	2,614.0	0.500	2,445,000 1,348,000 329,000	0.37	19,630	4.50 2.48 .606
	2	4.6 8.8 22.4	100,000	103.33	.0333	2,614.0	.500	2,445,000 1,169,000 342,500	.37	73,300	4.50 2.15 .630
Model B	1	2.8 4.7 5.7 7.1	44,860	65.43	.0470	3,090.0	.333	975,544 487,772 324,368 243,886	.25	56,436	4.00 2.00 1.33 1.00
	2	3.3 6.7 8.5 10.0	44,860	65.43	.0470	1,030.0	1.000	975,544 487,772 324,368 243,886	.25	56,436	4.00 2.00 1.33 1.00
Model C	1	3.7 10.0 20.0	100,000	106.38	.0343	2,972.9	.333	3,773,000 1,255,855 482,226	.25	25,233	6.94 2.31 .887
	2	10.0	100,000	106.38	.0343	2,256.3	.333	989,461	.25	25,233	1.82
	3	10.0	100,000	106.38	.0343	3,384.5	.333	1,440,699	.25	25,233	2.65
	4	10.0	100,000	106.38	.0343	4,512.7	.333	1,980,114	.25	25,233	3.64
Model D	1	4.3 10.3 20.5	62,500	50.23	.0258	2,239.0	.333	1,450,893 428,132 155,962	.25	12,406	4.27 1.26 .459
	2	3.9 10.1 20.2	102,000	154.48	.0487	1,885.4	.333	2,168,225 720,893 273,939	.25	12,406	3.91 1.30 .494

NATIONAL ADVISORY COMMITTEE FOR AERONAUTICS

TABLE IV

MOST SERIOUS VALUES OF OVERSTRESS FROM ADDING THE REACTIONS OF TWO GUSTS

[Based on reference 11]

H_1 (chords)	H_2 (chords)	H_3 (chords)	$\frac{\delta_{d_{max}}}{\delta_{st}}$
Model C, condition 1			
3.75	3.75	16.23	1.40
3.75	9.99	13.74	1.26
3.75	19.98	3.75	1.26
9.99	3.75	39.94	1.35
9.99	9.99	37.46	[a]1.25
9.99	19.98	27.47	1.08
19.98	3.75	72.43	1.44
19.98	9.99	69.93	1.34
19.98	19.98	59.94	1.20
Model D, condition 1			
4.26	4.26	14.50	1.20
4.26	10.25	11.96	1.09
4.26	19.53	5.13	1.09
10.25	4.26	35.04	1.31
10.25	10.25	32.48	[a]1.21
10.25	19.53	25.64	1.20
19.53	4.26	69.22	1.42
19.53	10.25	66.66	1.34
19.53	19.53	59.82	1.39
Model D, condition 2			
3.96	3.96	15.47	1.47
3.96	10.08	13.31	1.35
3.96	20.15	11.87	1.35
10.08	3.96	35.98	1.47
10.08	10.08	33.83	[a]1.26
10.08	20.15	32.39	1.11
20.15	3.96	73.41	1.56
20.15	10.08	71.25	1.36
20.15	20.15	69.81	1.23

[a]Used in extended analysis of repeated gusts.

NATIONAL ADVISORY
COMMITTEE FOR AERONAUTICS

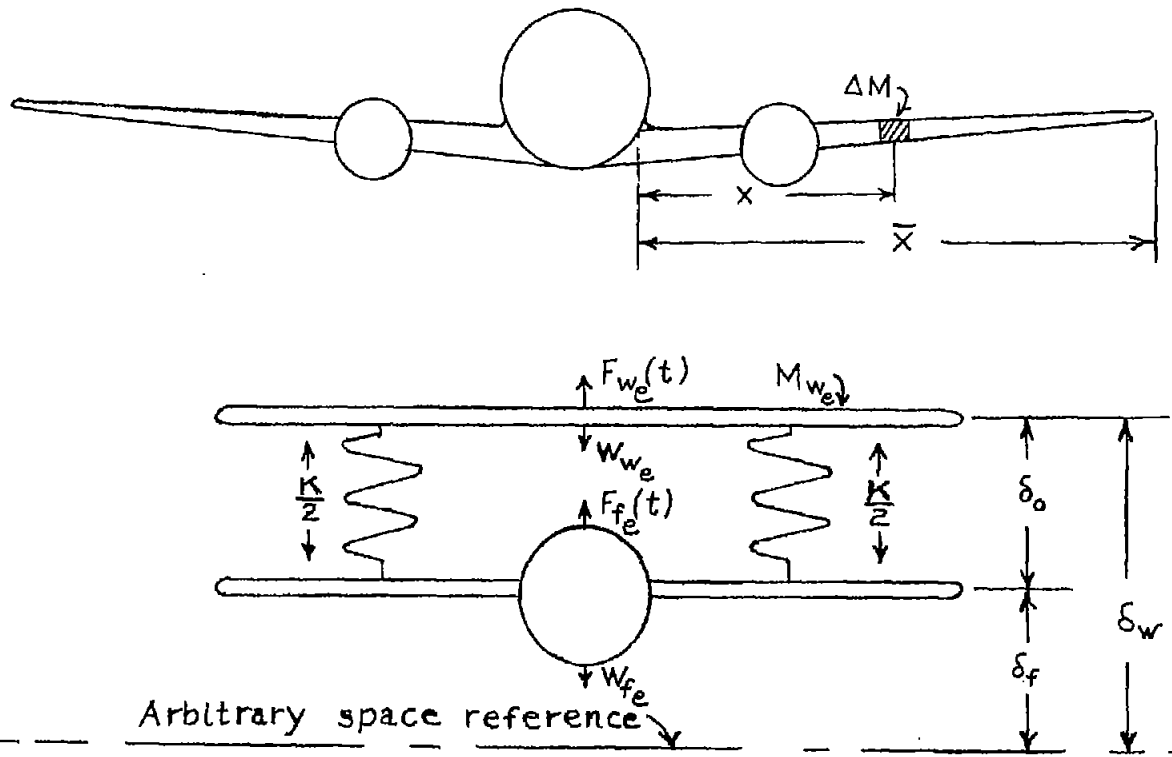

In the calculations δ_o is disregarded and in level-flight condition $\delta_w - \delta_f = 0$

NATIONAL ADVISORY COMMITTEE FOR AERONAUTICS

Figure 1.- Equivalent biplane.

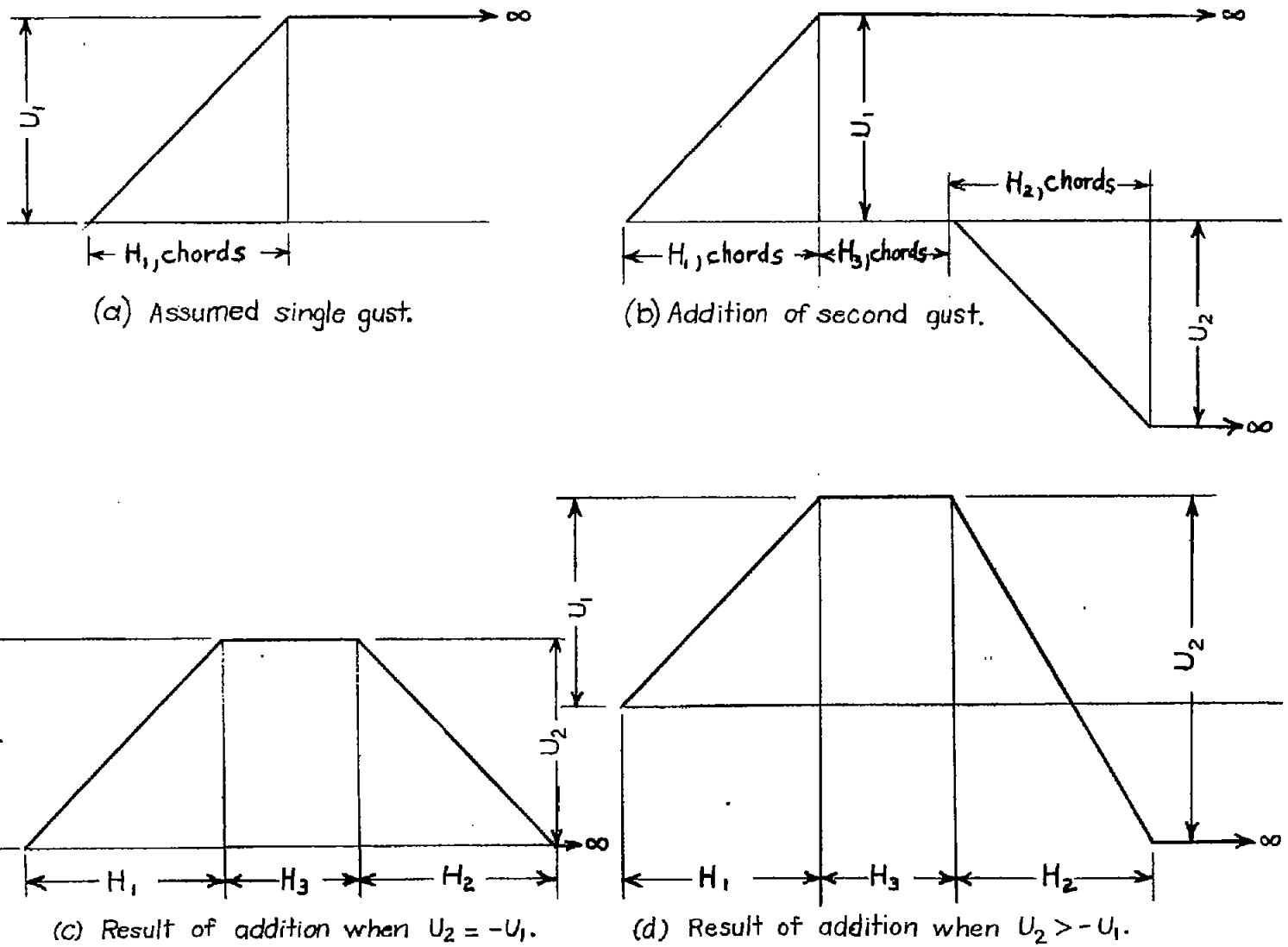

Figure 2.- Addition of gusts.

NATIONAL ADVISORY COMMITTEE FOR AERONAUTICS

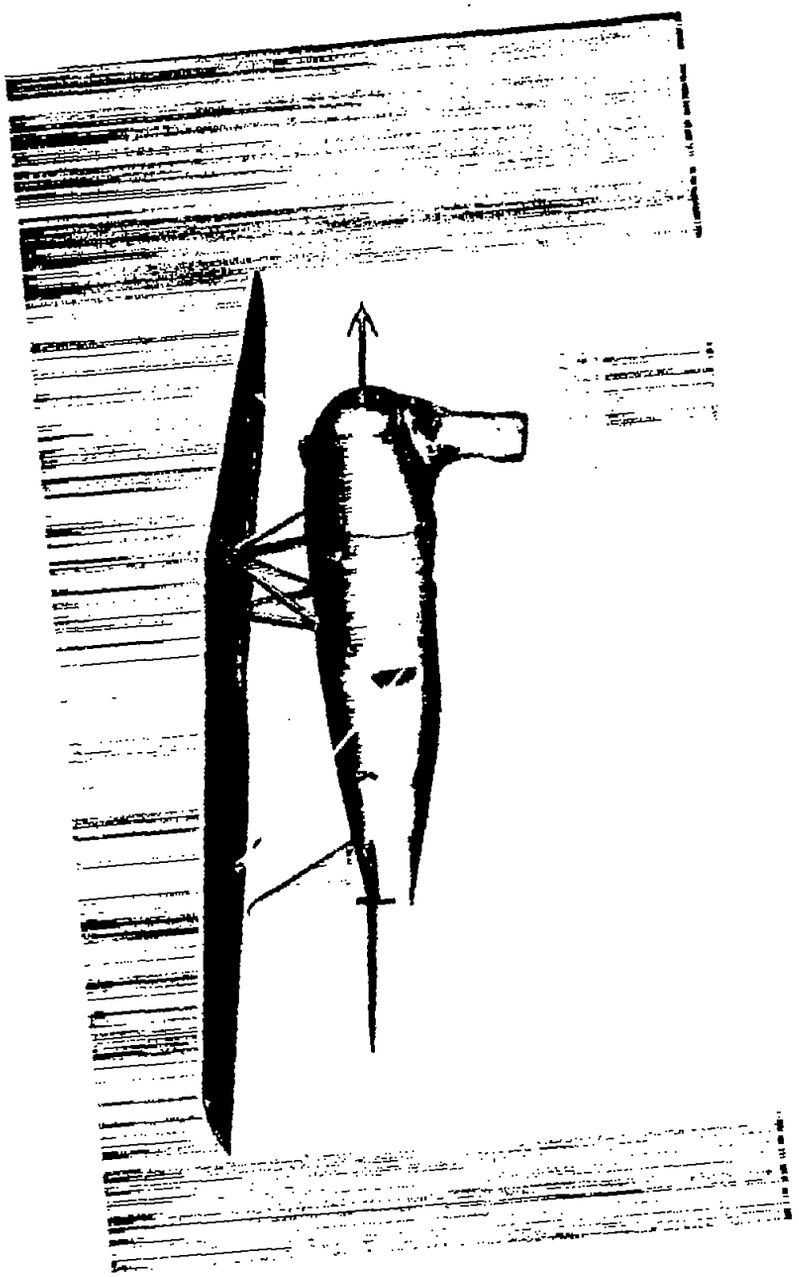

Figure 3.- Test model.

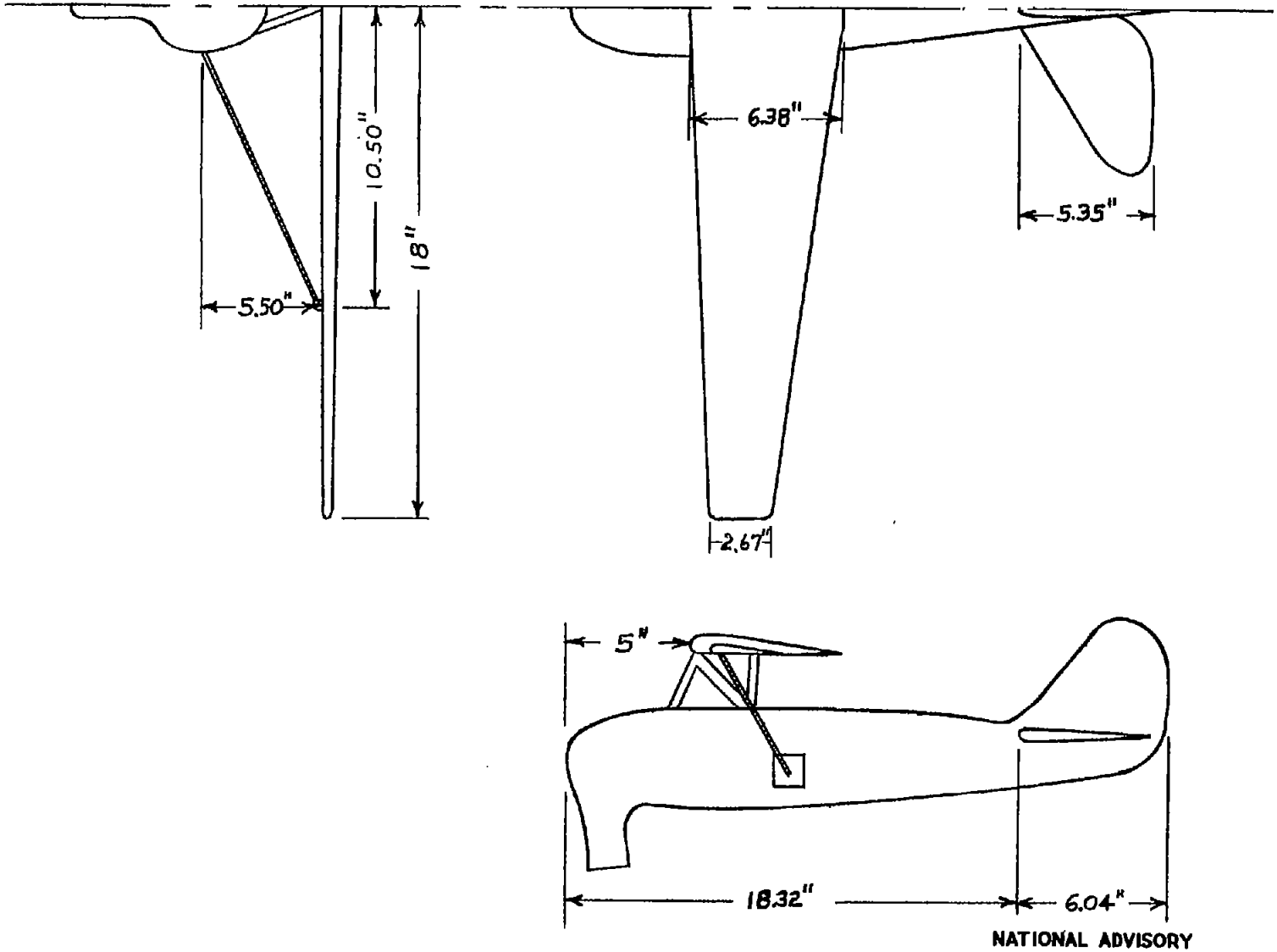

Figure 4.-Line drawing of test model.

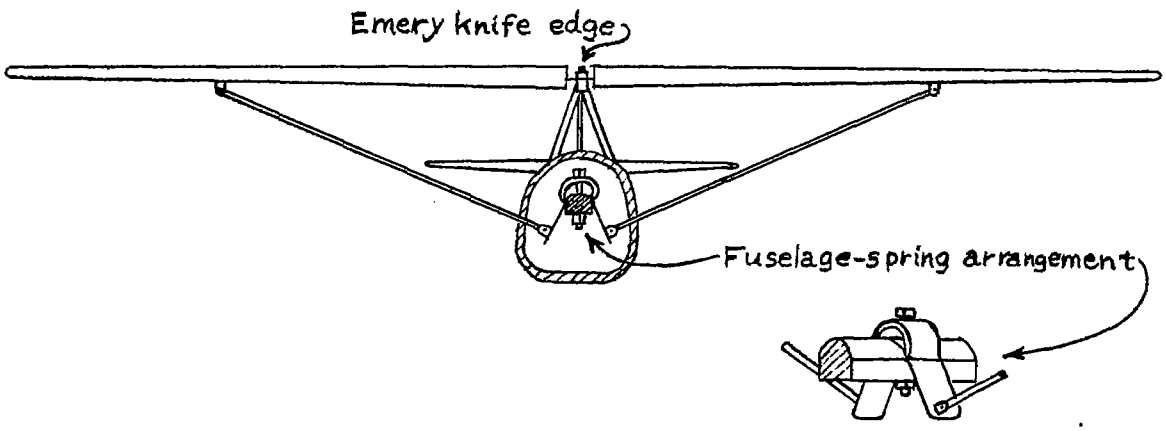

Figure 5.- Diagram of knife edge, struts, and fuselage spring of test model.

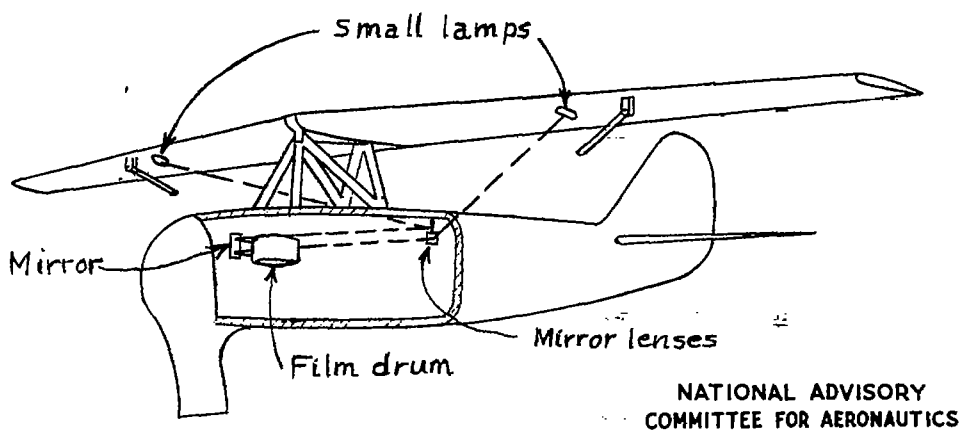

Figure 6.- Method of measuring wing deflection.

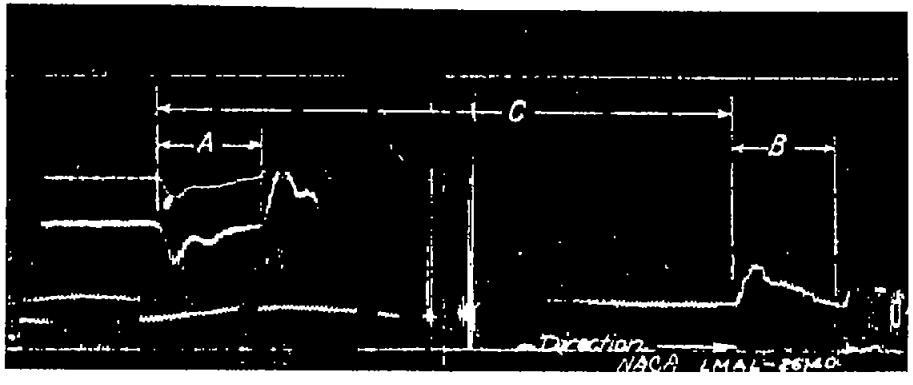

Figure 7.- Instrument record showing A, wing-tip-deflection time histories, B, accelerometer time history, and C, distance between A and B resulting from the record light beams striking the film 90° apart on the drum.

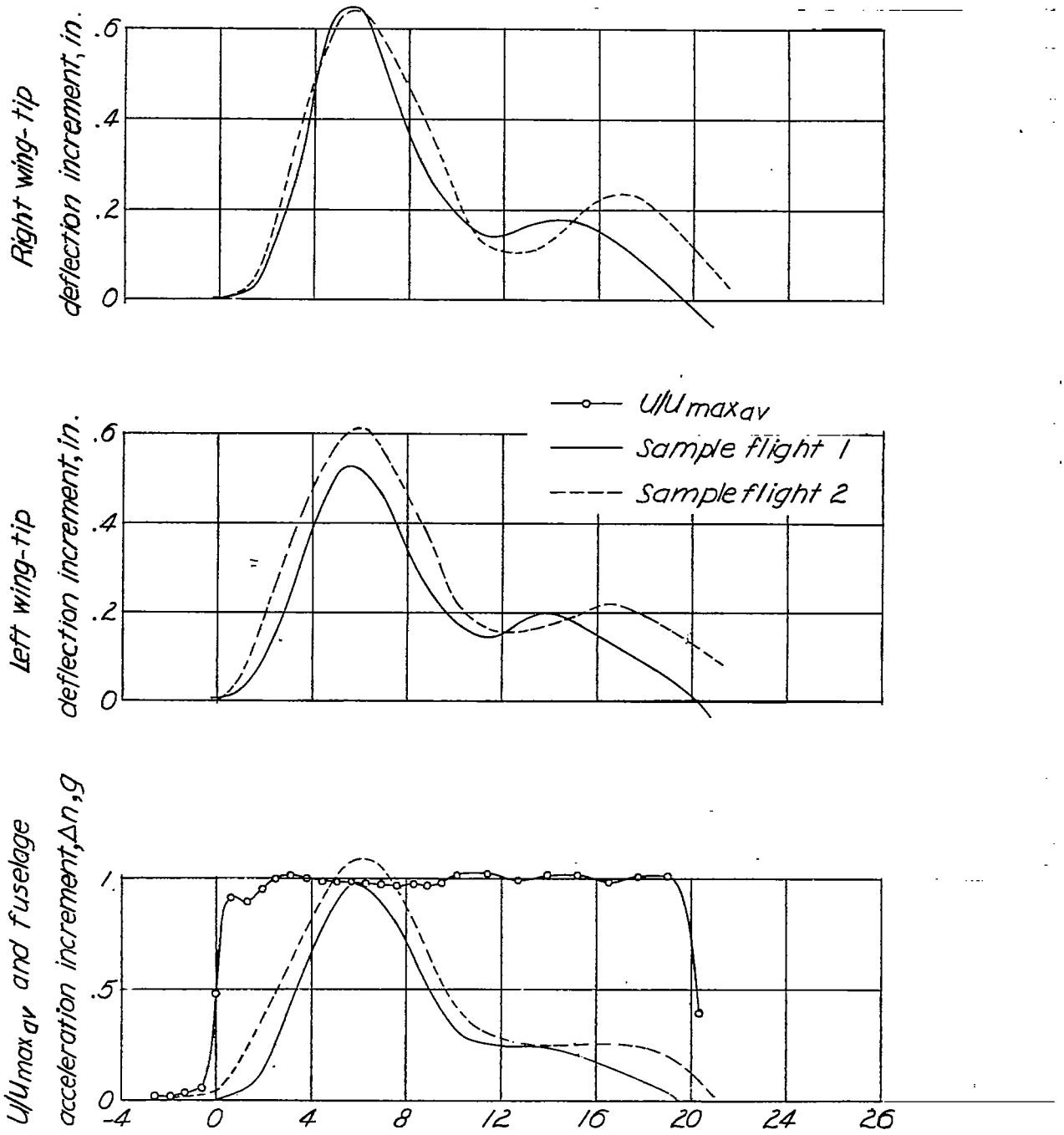

(a) Sharp-edge gust with 2.4-chord gradient distance.

Figure 8.-History of events. f=13.5cps.

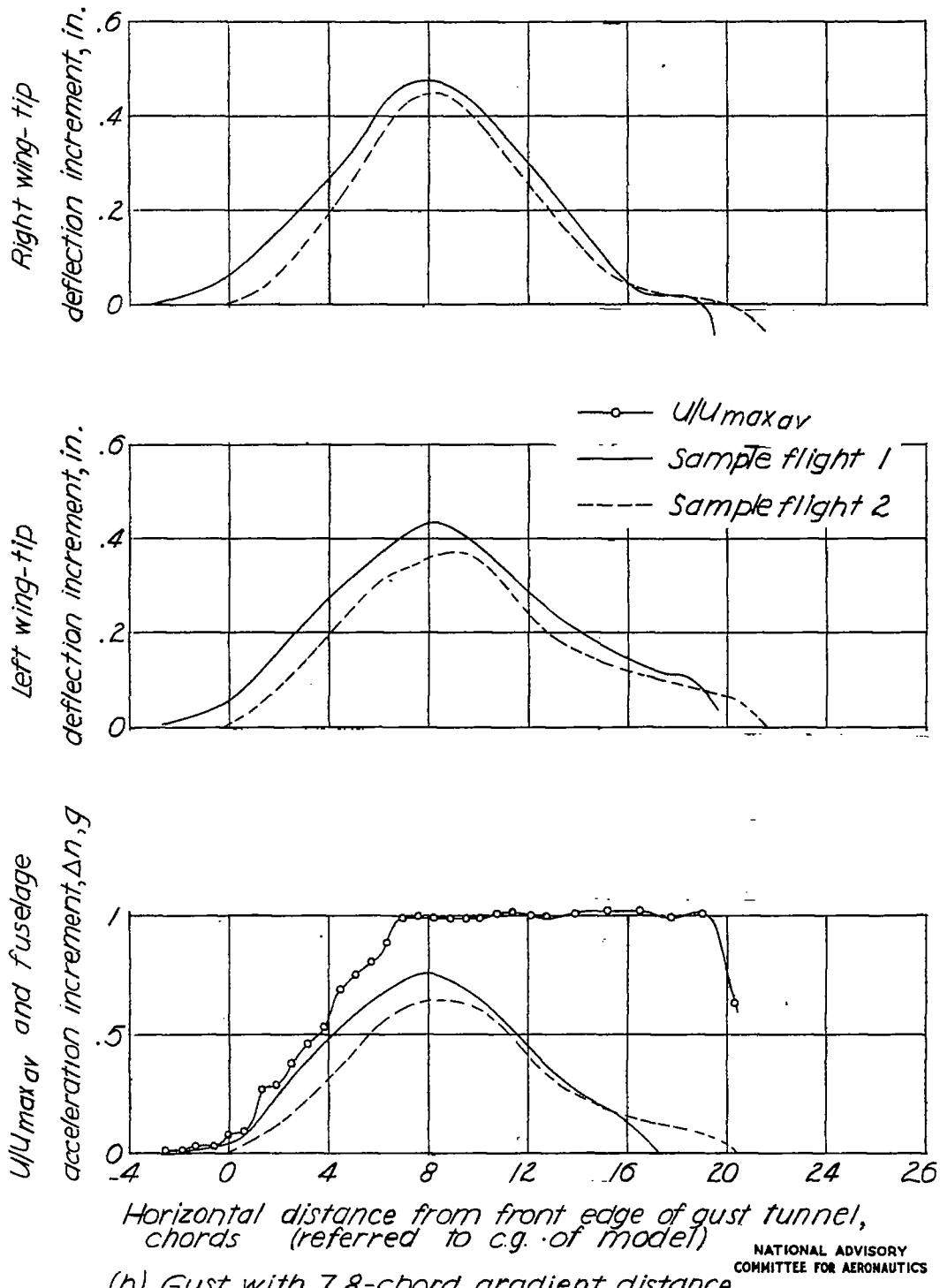

(b) Gust with 7.8-chord gradient distance.

Figure 8. - Continued.

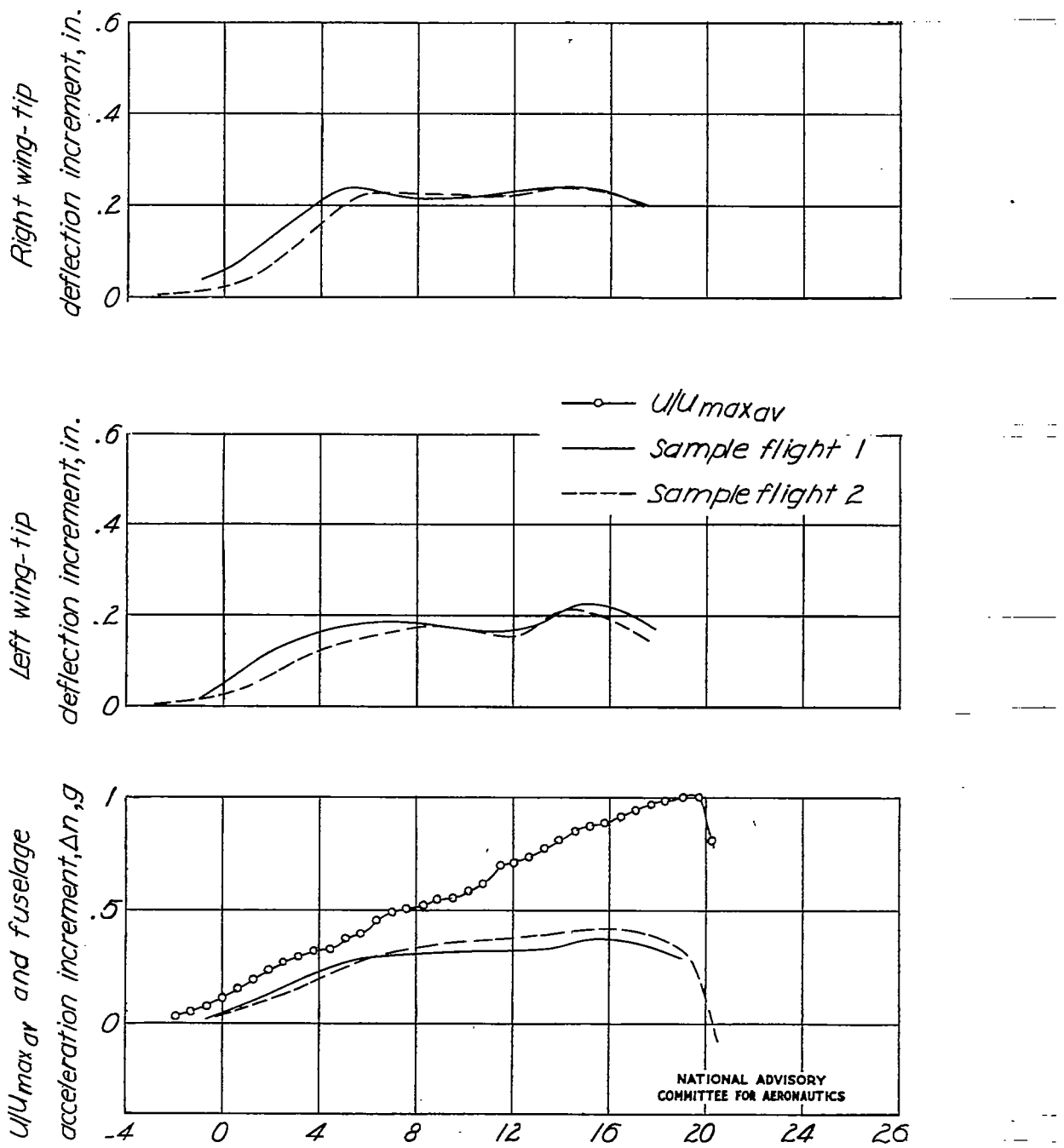

(c) Gust with 21.2-chord gradient distance.

Figure 8.-Concluded.

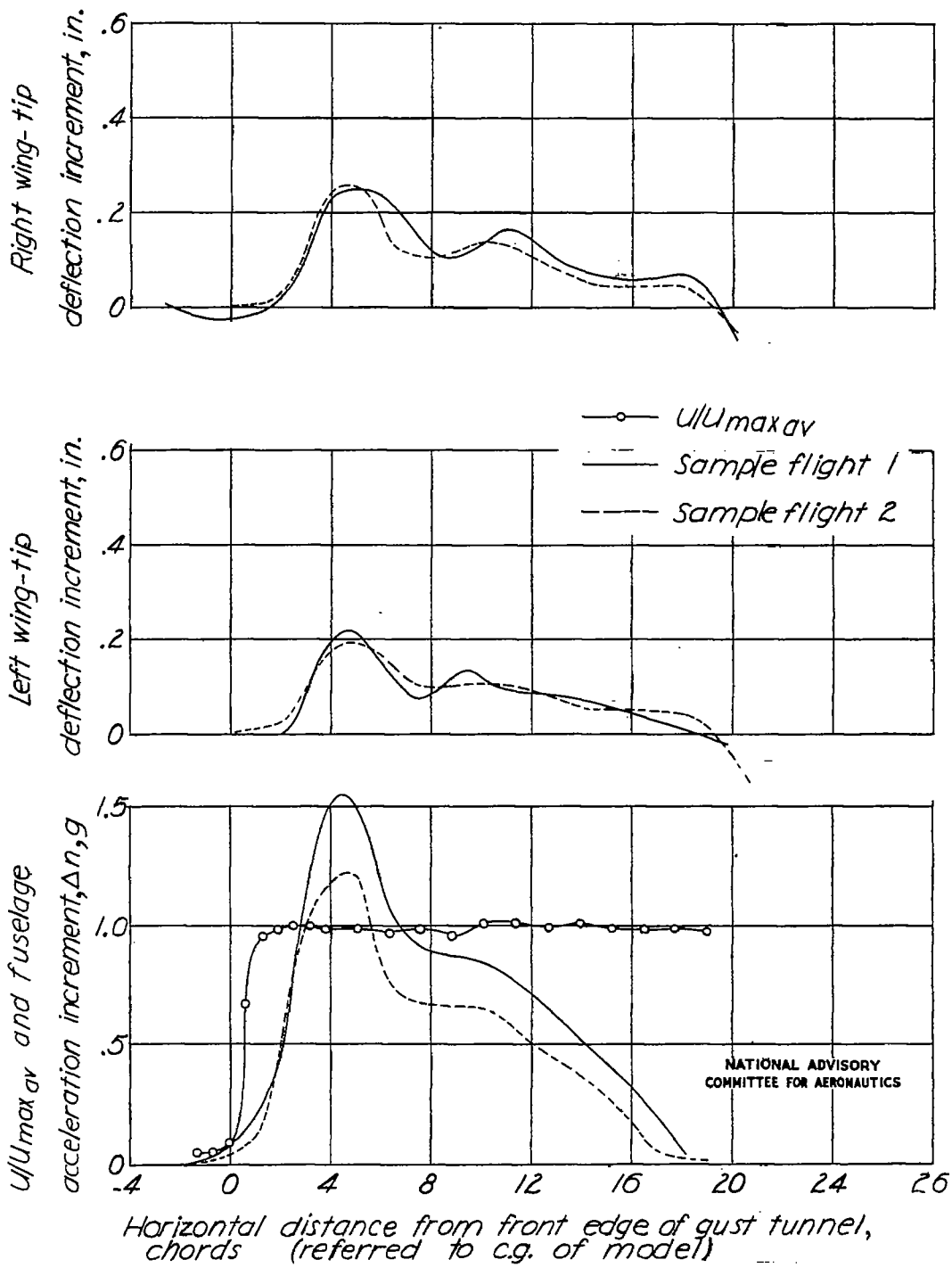

(a) Sharp-edge gust with 1.8-chord gradient distance.

Figure 9.-History of events, f = 26.1 cps.

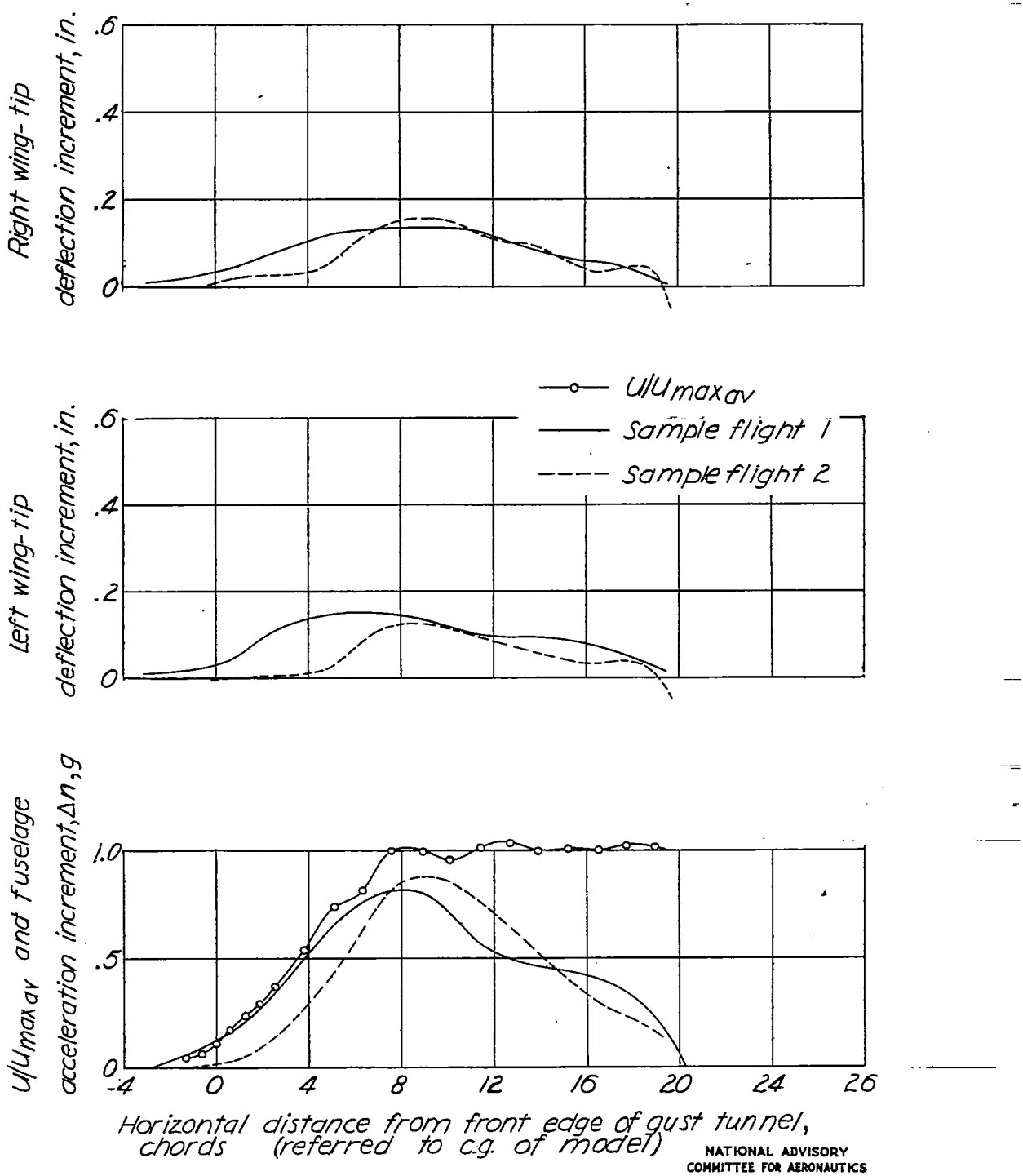

(b) Gust with 8.8-chord gradient distance.

Figure 9. - Continued.

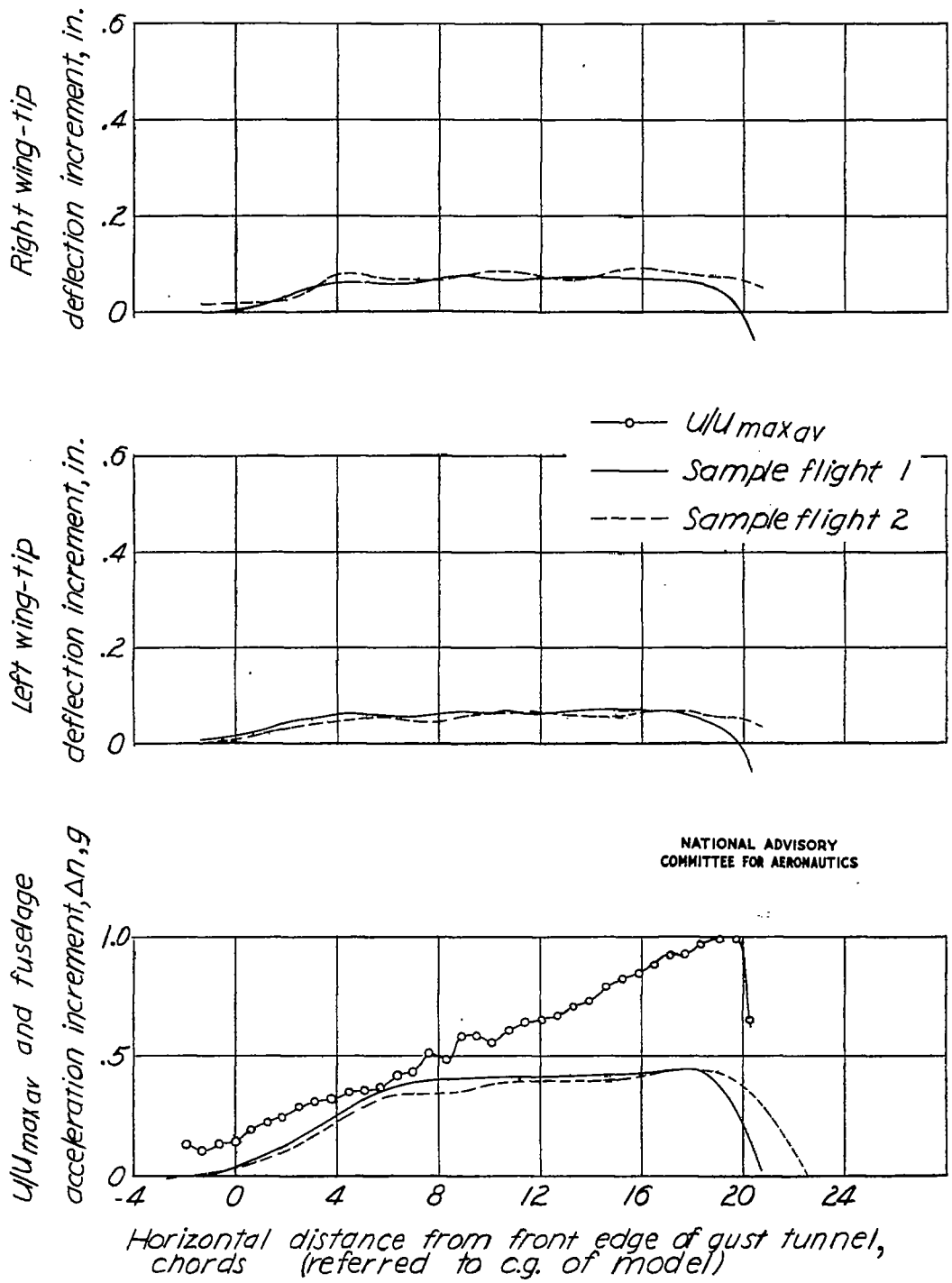

(c) Gust with 22.4-chord gradient distance.

Figure 9. - Concluded.

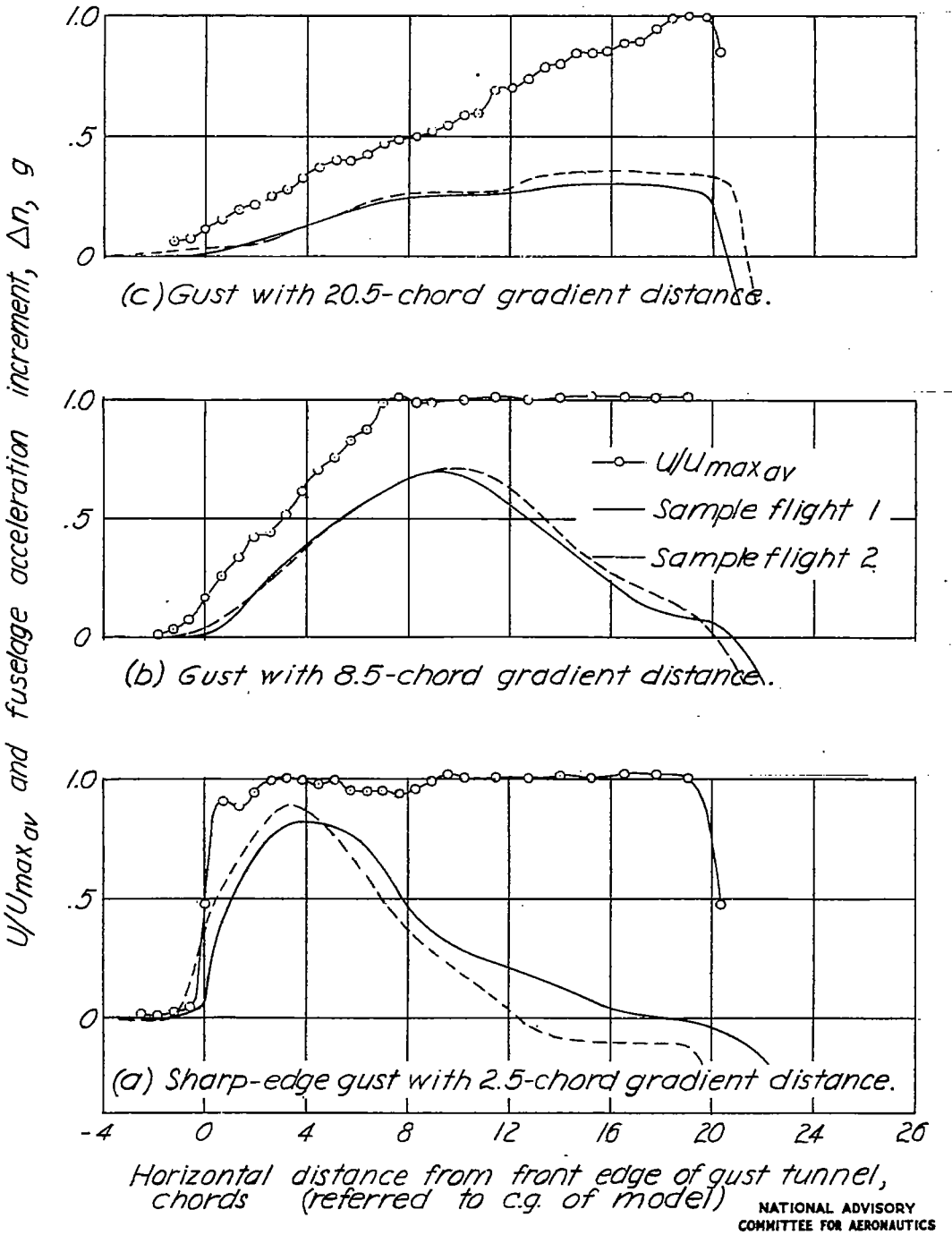

Figure 10.- History of events. Rigid model.

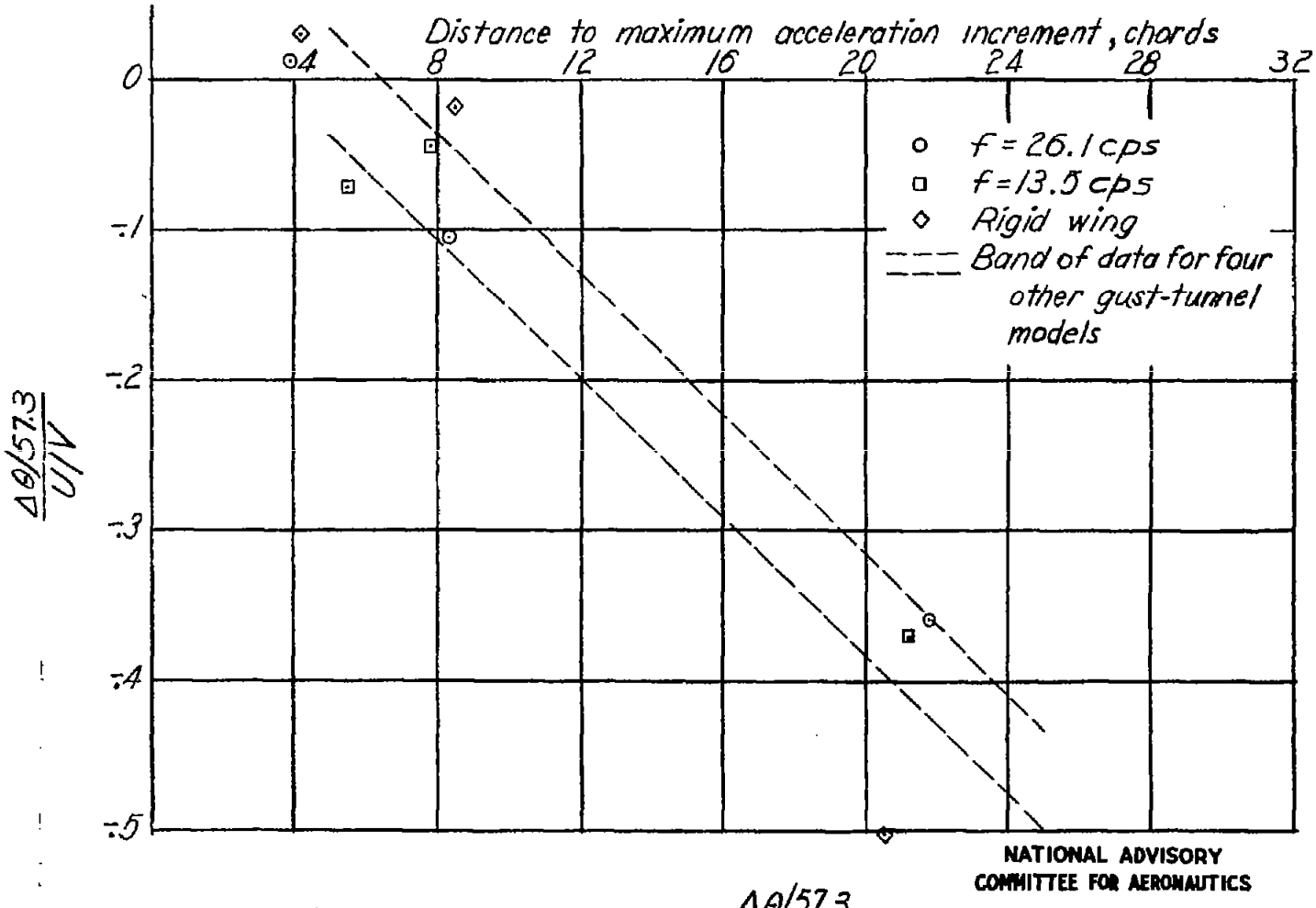

Figure 11.—Variation of experimental $\frac{\Delta\theta/57.3}{U/V}$ with distance to maximum acceleration increment for three conditions of test model and for four other gust-tunnel models.

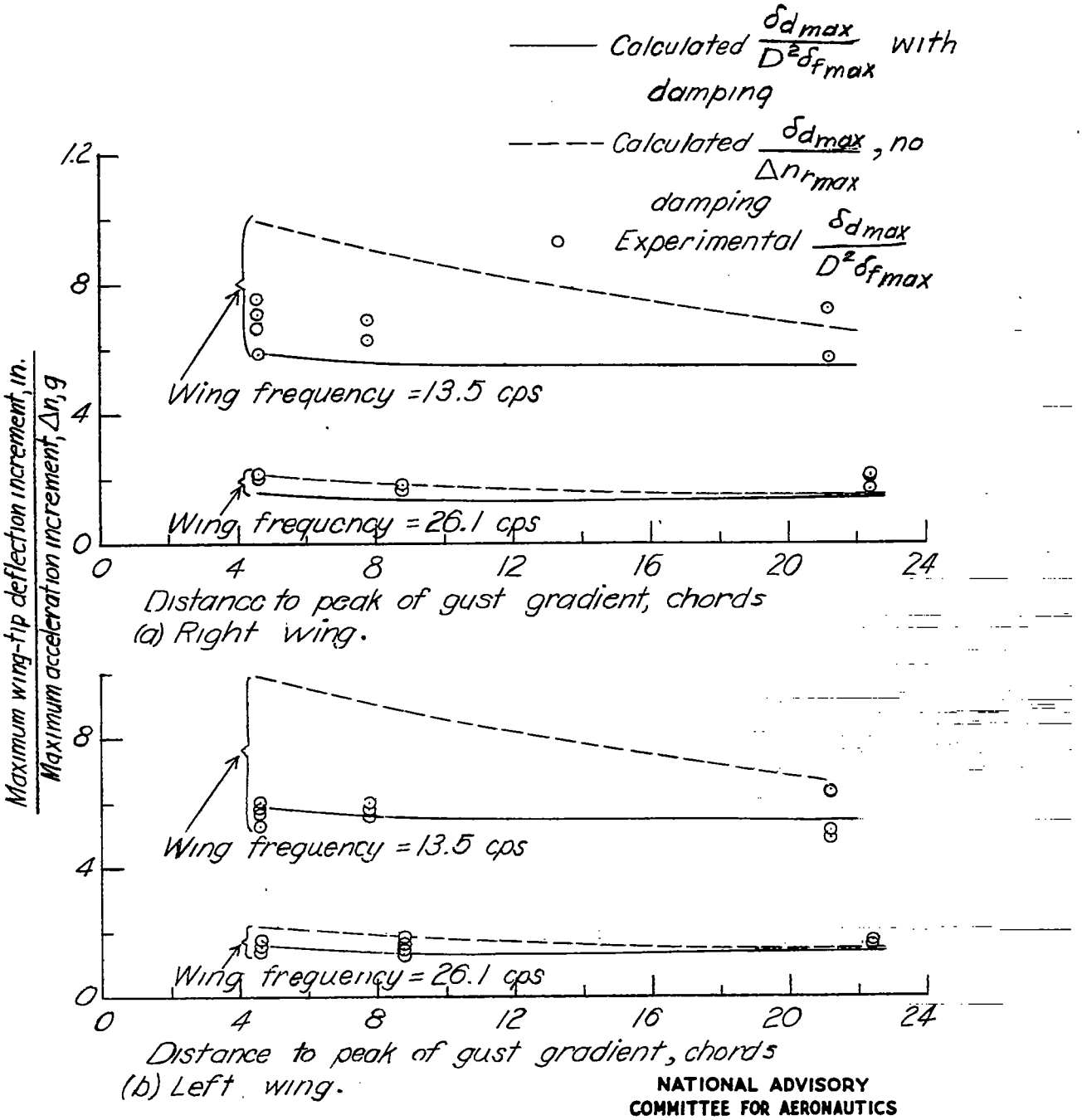

Figure 12.- Comparison of calculated and experimental values of $\frac{\text{maximum wing-tip deflection increment}}{\text{maximum acceleration increment}}$ for change in gradient distance.

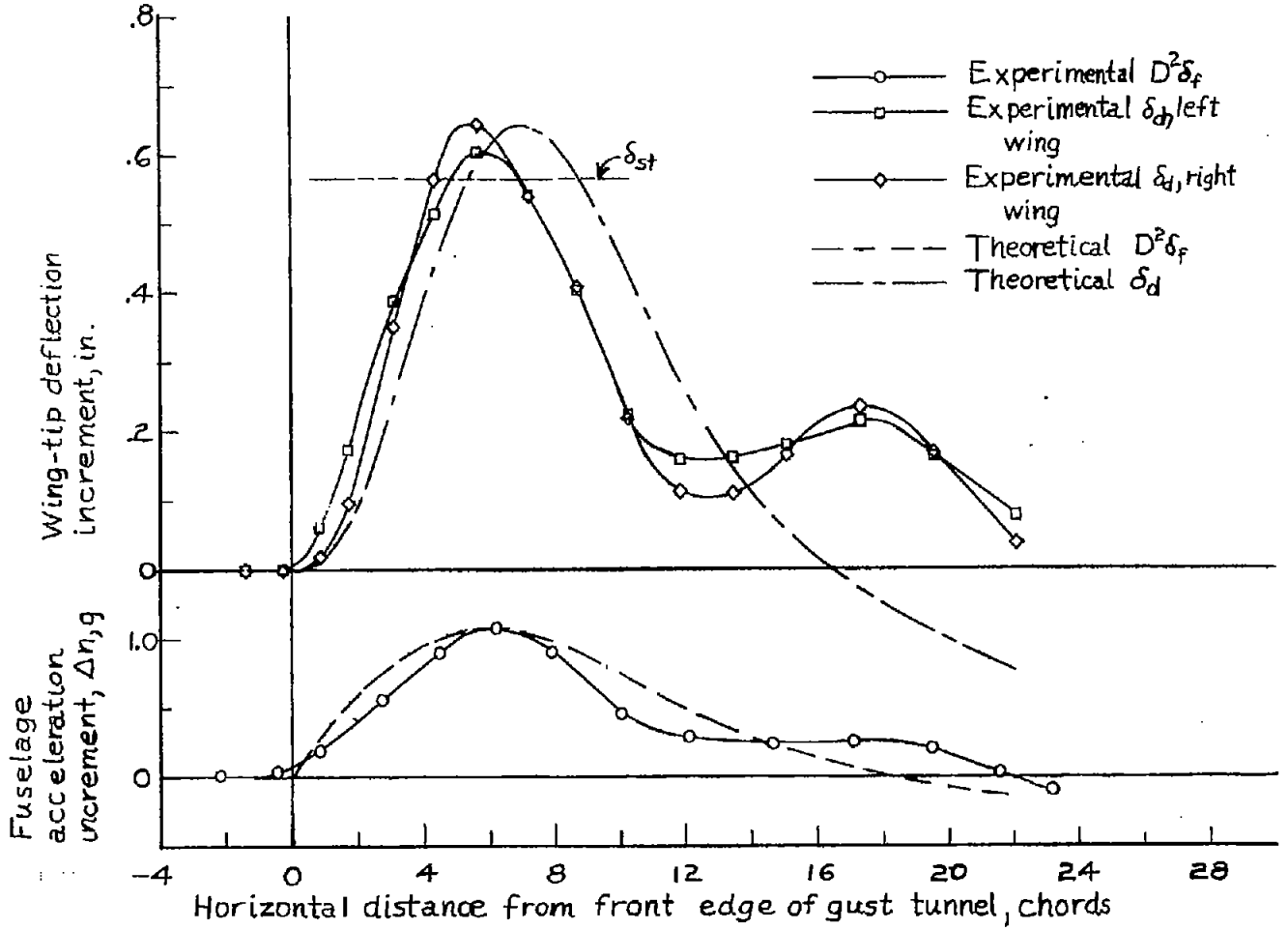

(a) Sharp-edge gust with 2.4-chord gradient distance. Sample flight 2.

Figure 13.— Comparison of experimental and theoretical reactions to a gust. f = 13.5 cps.

NATIONAL ADVISORY
COMMITTEE FOR AERONAUTICS

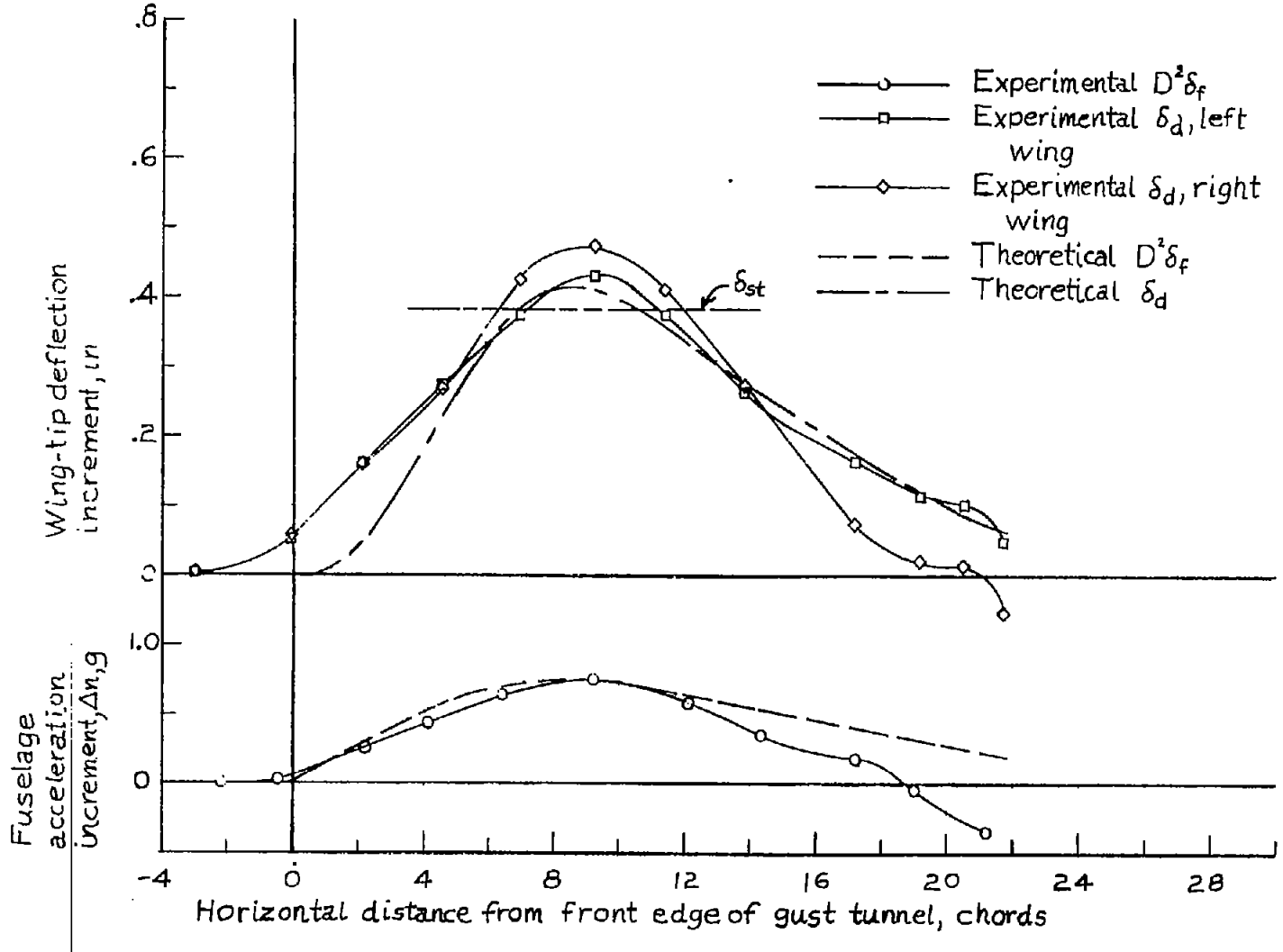

(b) Gust with 7.8-chord gradient distance. Sample flight 1.

Figure 13.— Continued.

NATIONAL ADVISORY COMMITTEE FOR AERONAUTICS

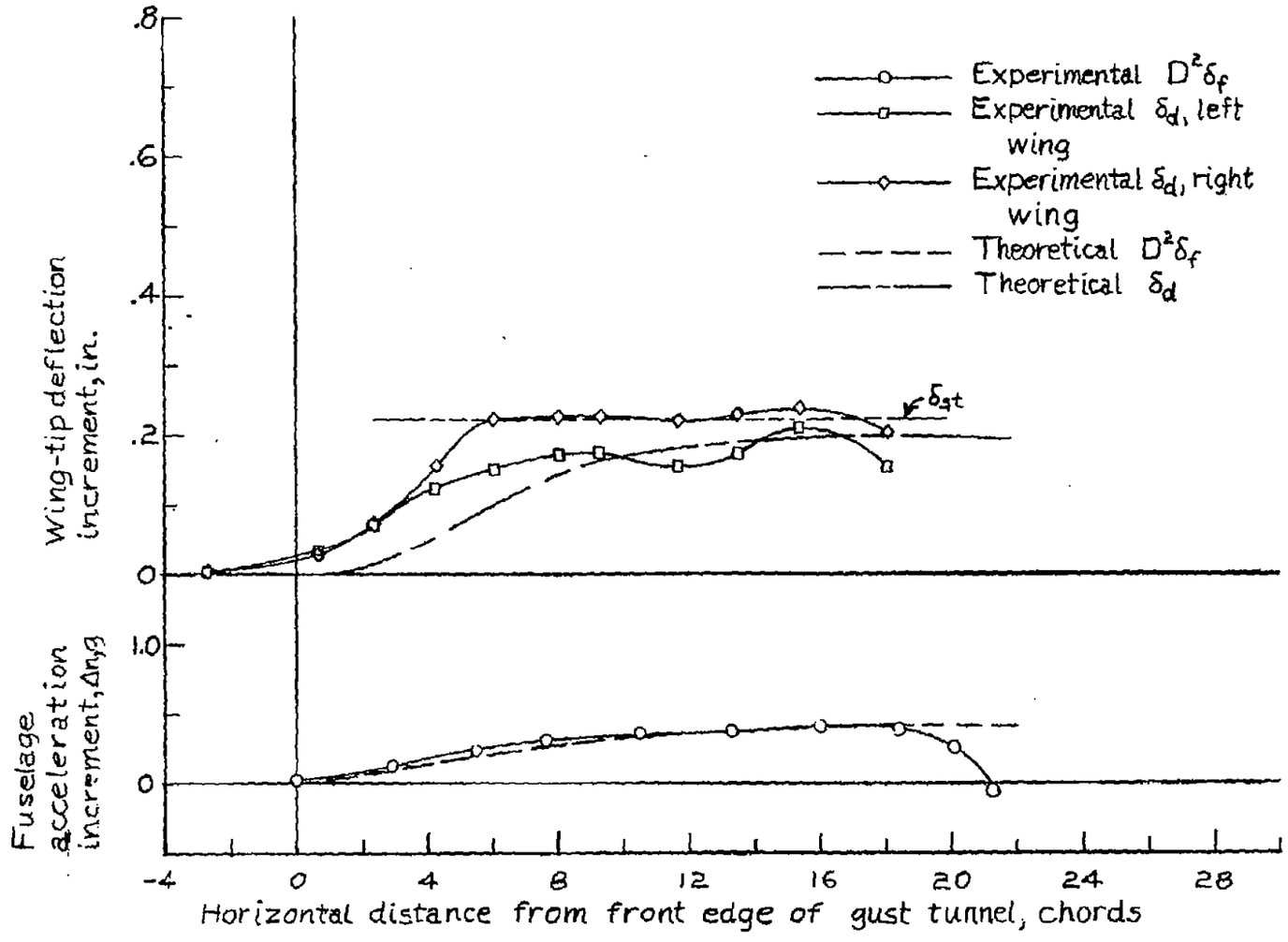

(c) Gust with 21.2-chord gradient distance. Sample flight 2.

Figure 13.— Concluded.

NATIONAL ADVISORY COMMITTEE FOR AERONAUTICS

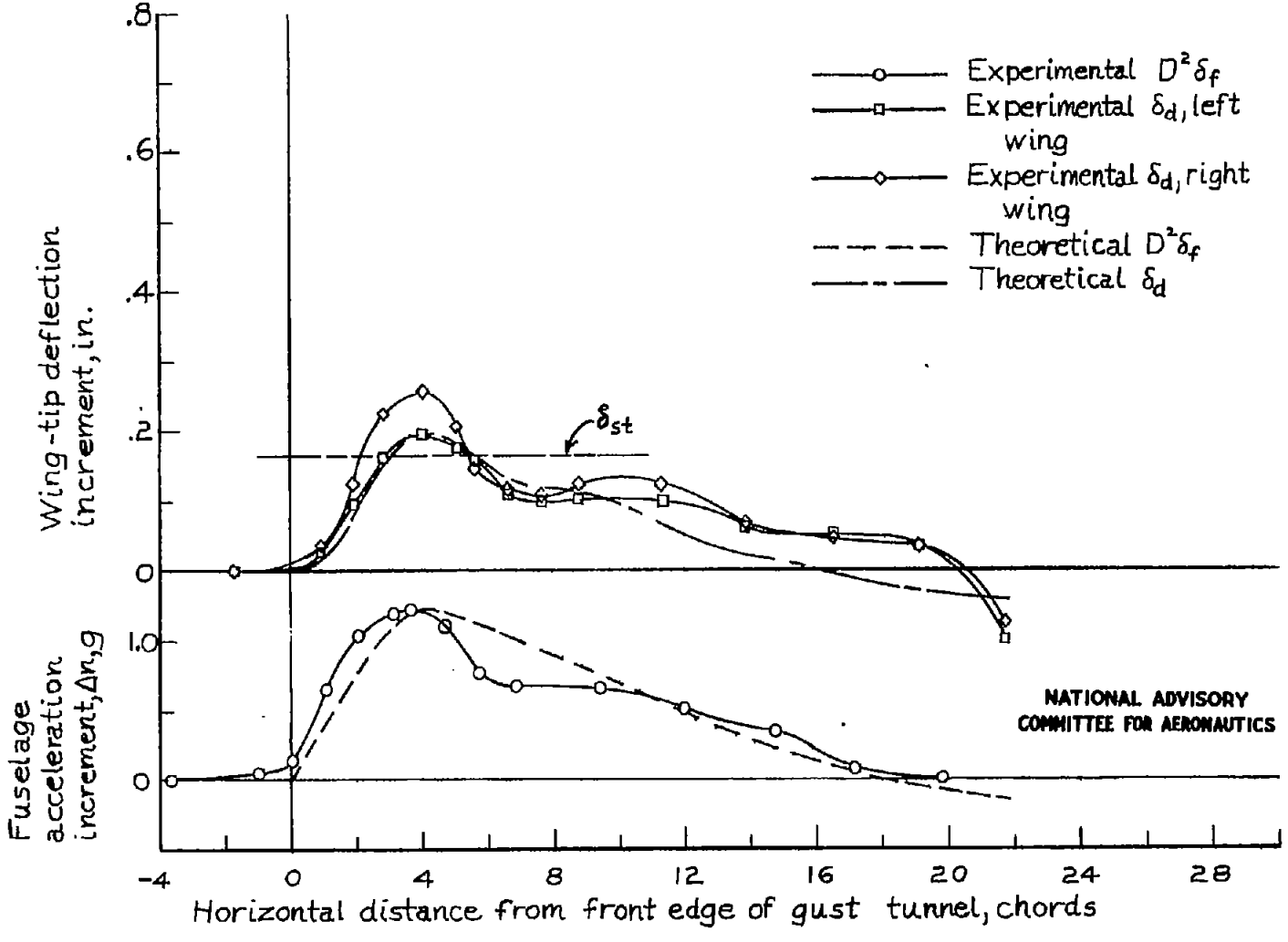

(a) Sharp-edge gust with 1.8-chord gradient distance. Sample flight 2.

Figure 14.— Comparison of experimental and theoretical reactions to a gust. f = 26.1 cps.

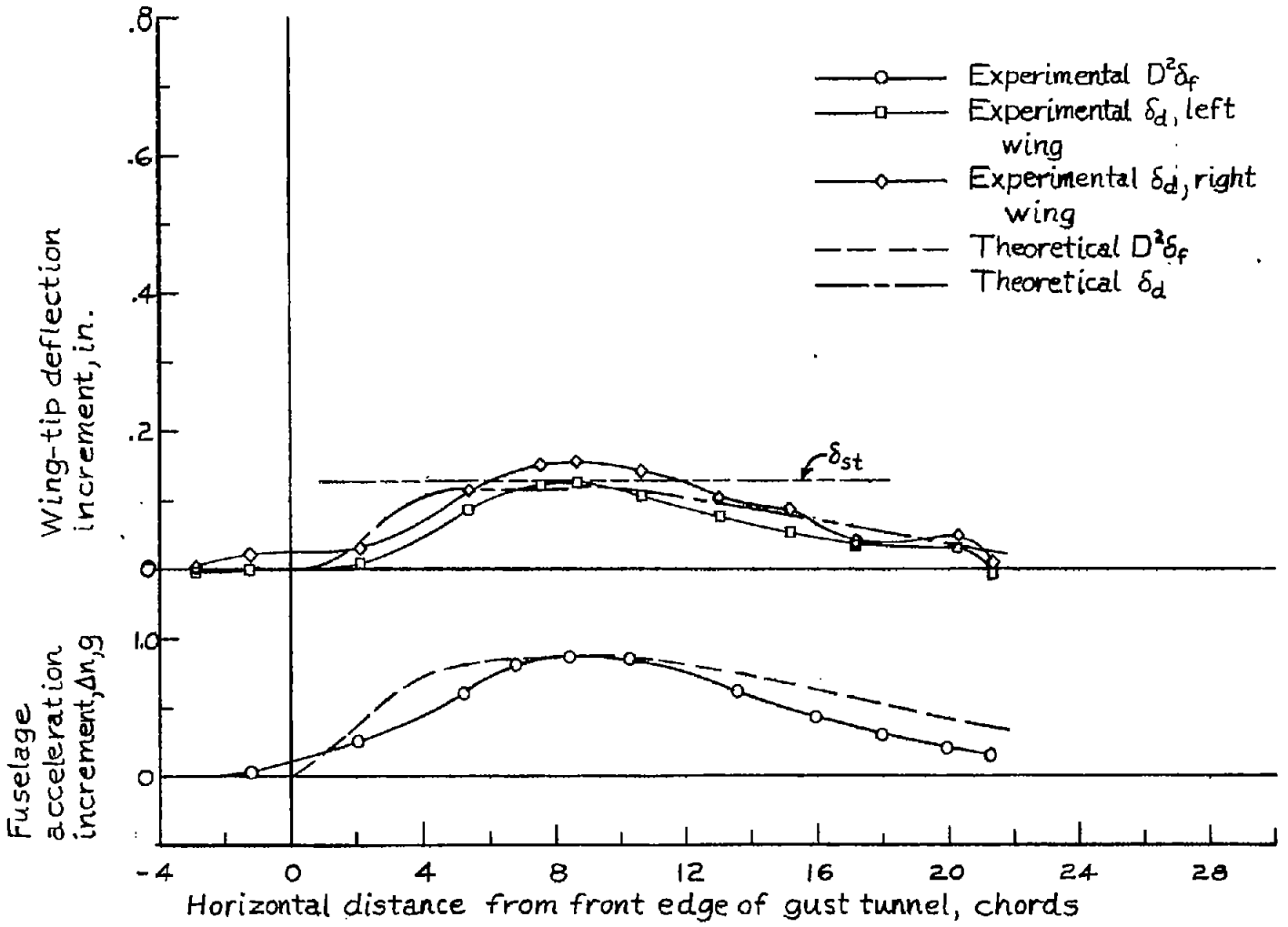

(b) Gust with 8.8-chord gradient distance. Sample flight 2.

Figure 14.— Continued.

NATIONAL ADVISORY COMMITTEE FOR AERONAUTICS

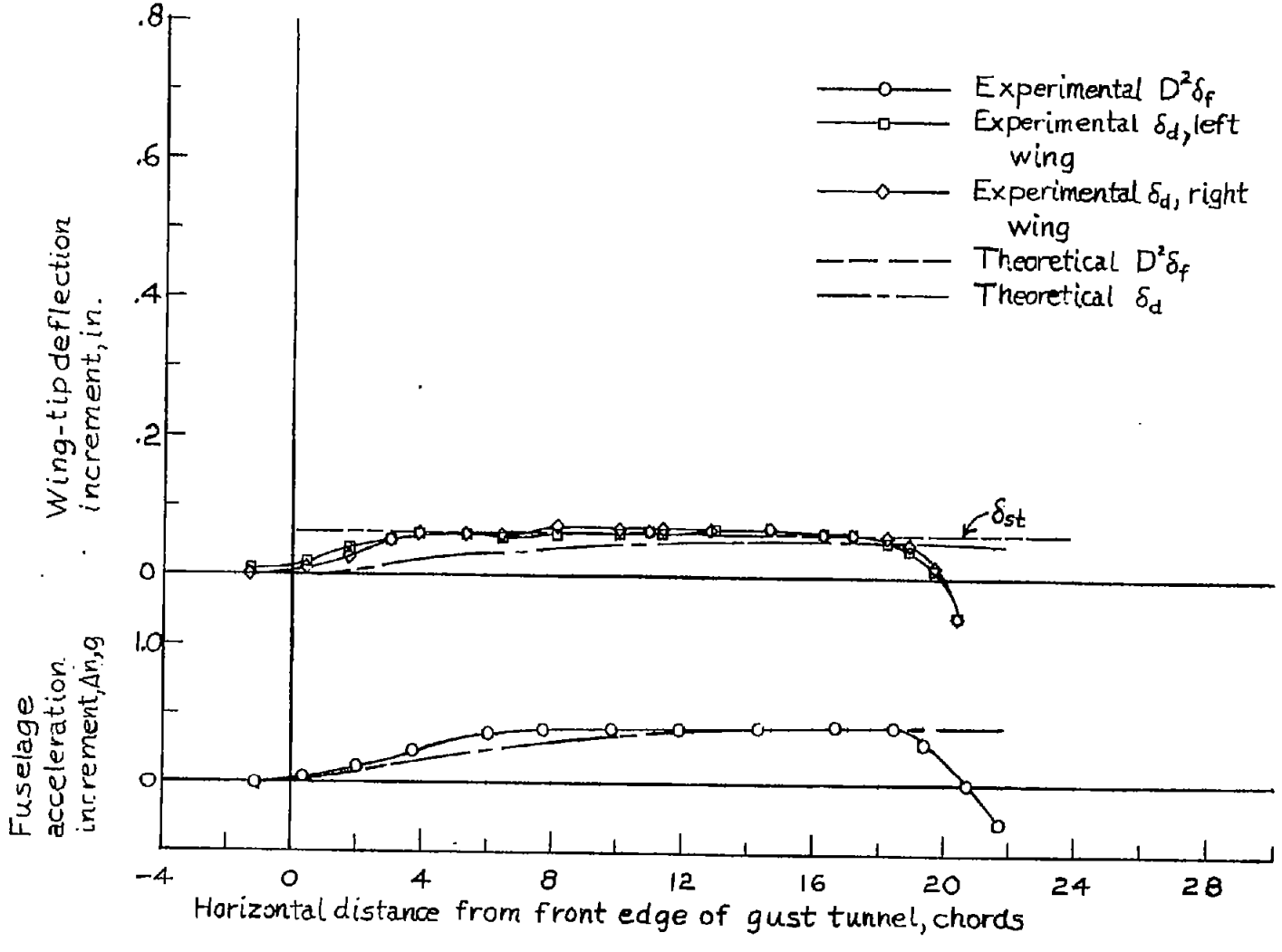

(c) Gust with 22.4-chord gradient distance. Sample flight 1.

Figure 14.— Concluded.

NATIONAL ADVISORY COMMITTEE FOR AERONAUTICS

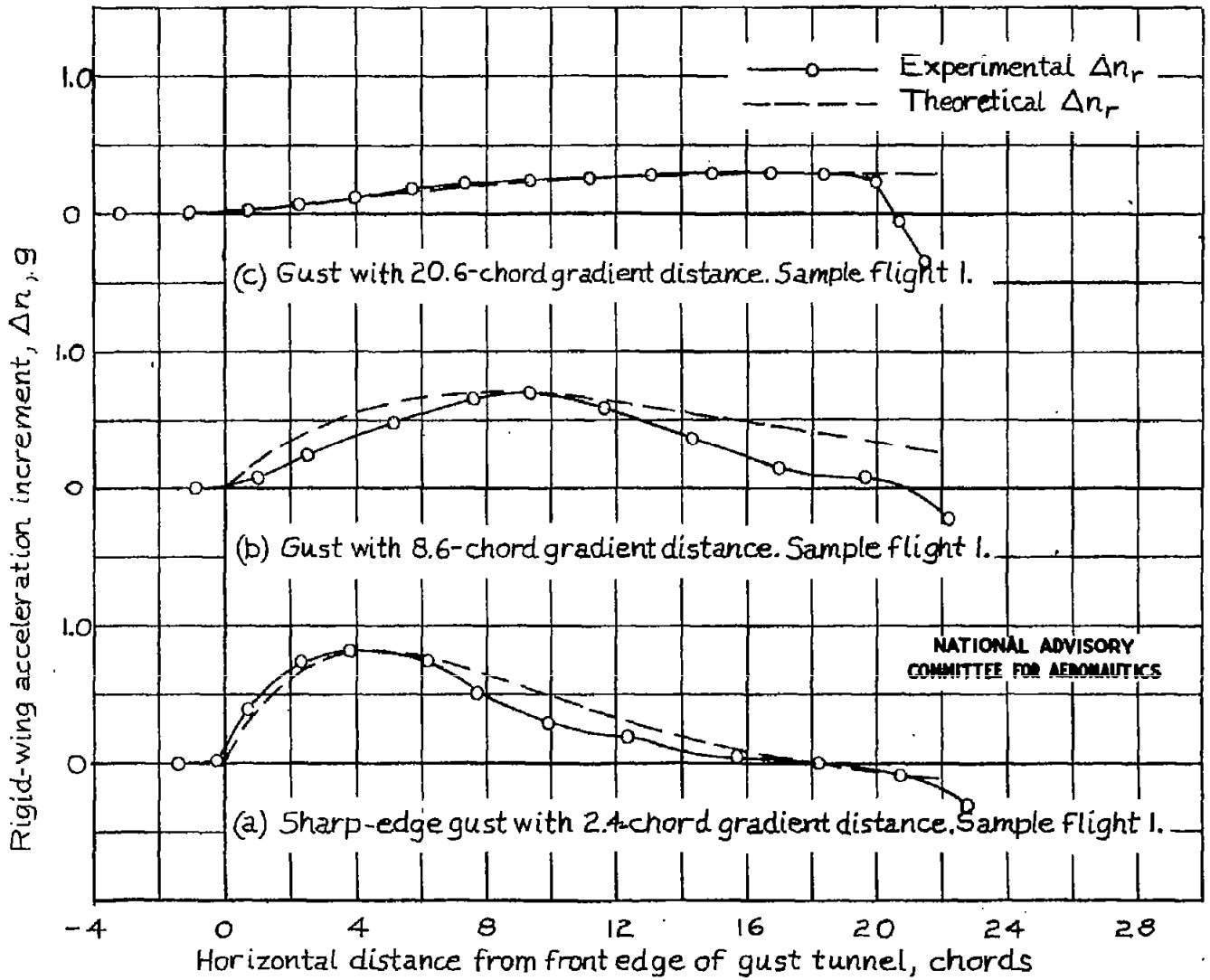

Figure 15 .— Comparison of experimental and theoretical reactions to a gust. Rigid wings.

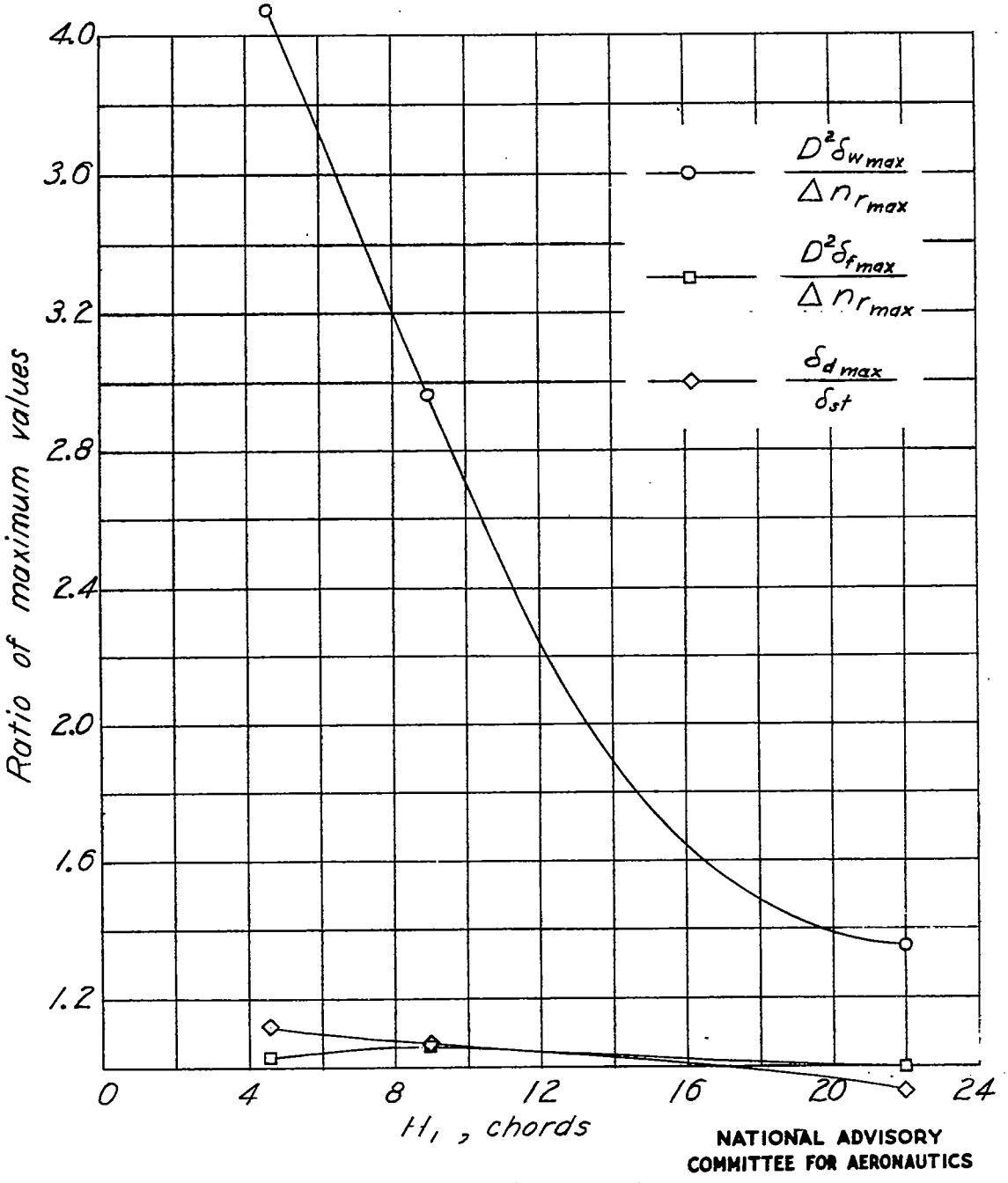

(a) Model A, condition 1.

Figure 16.–Variations of ratios of maximum dynamic to static response with gradient distance.

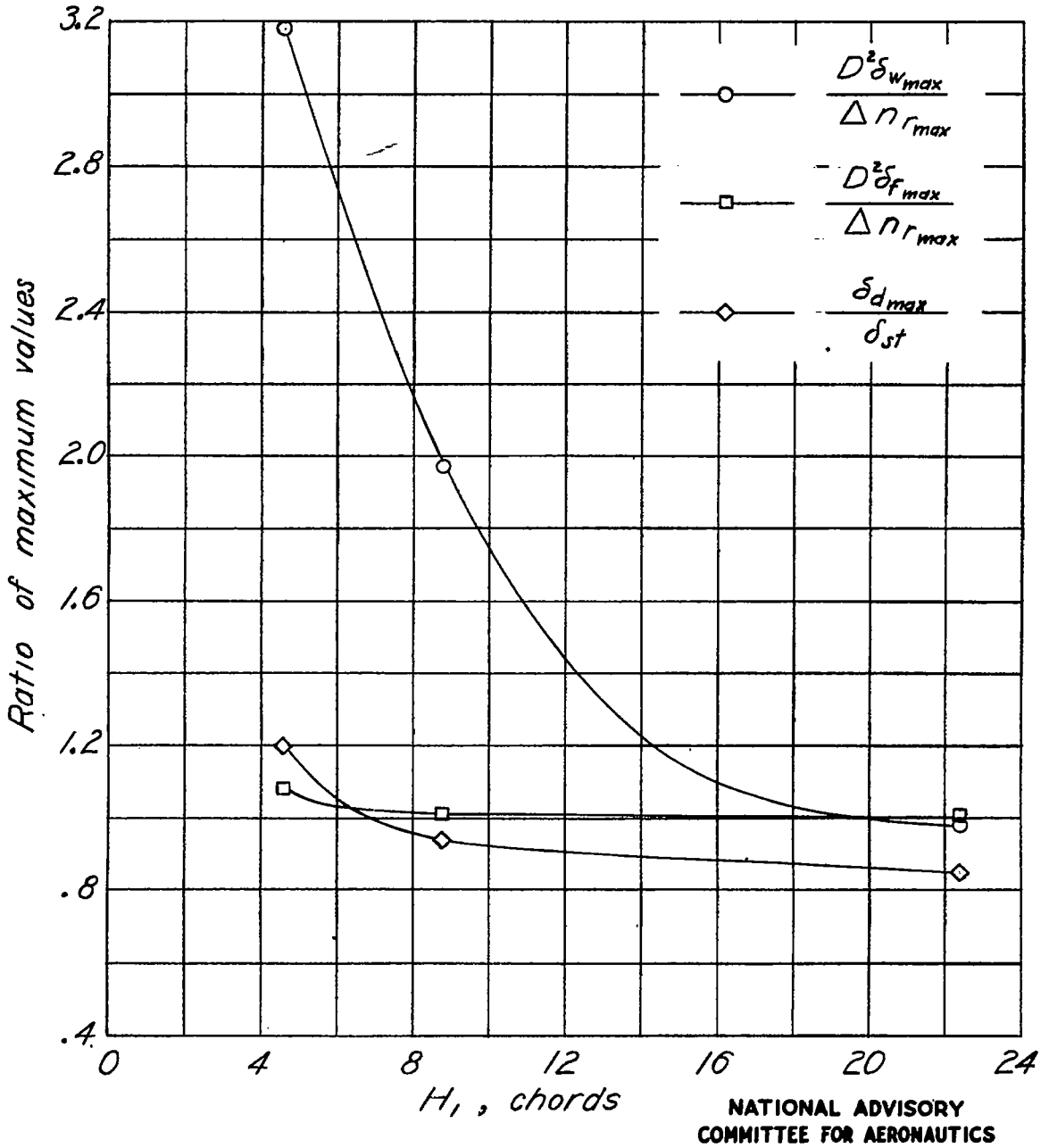

(b) Model A, condition 2.

Figure 16 - Continued.

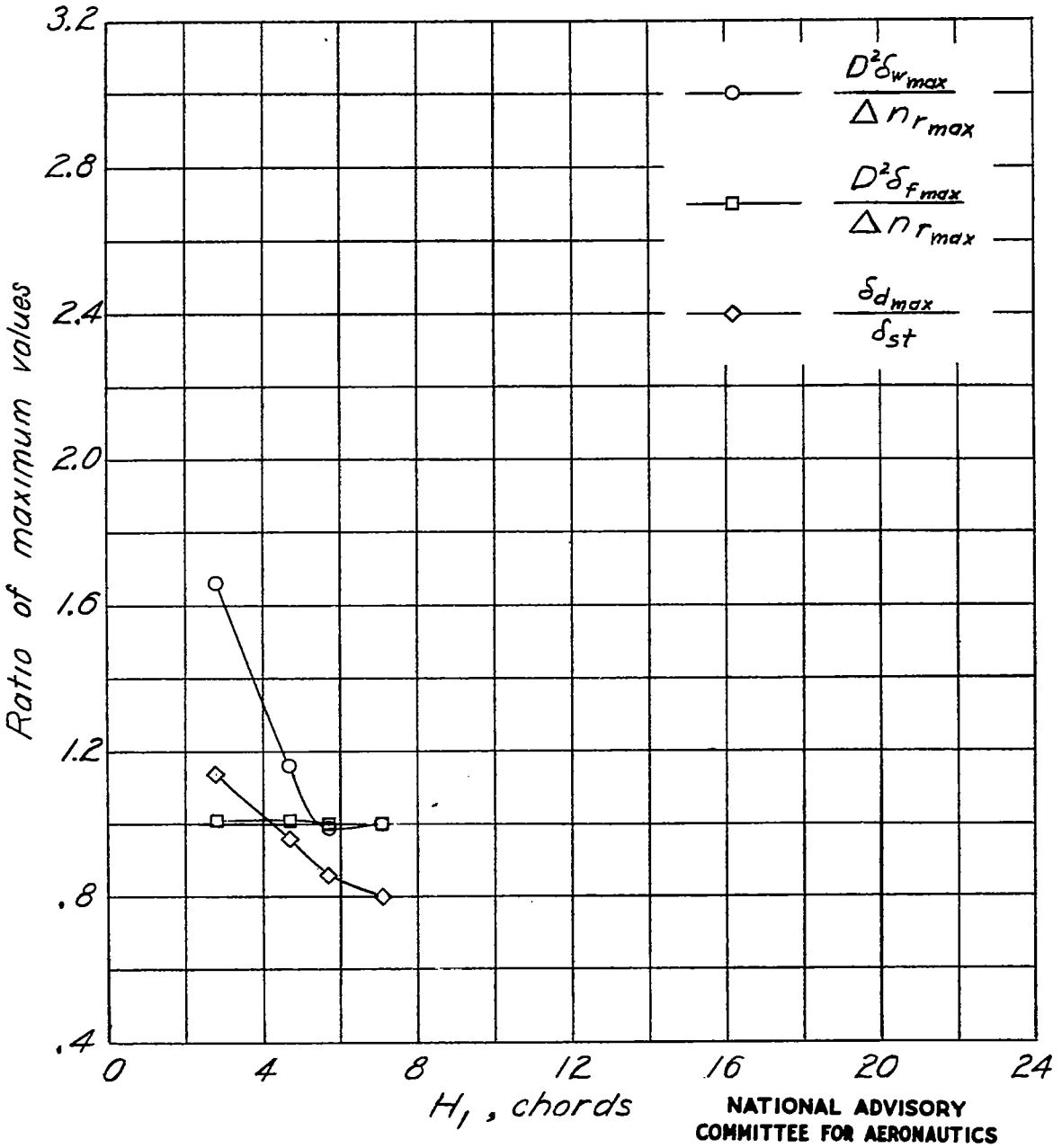

(c) Model B, condition 1

Figure 16.- Continued.

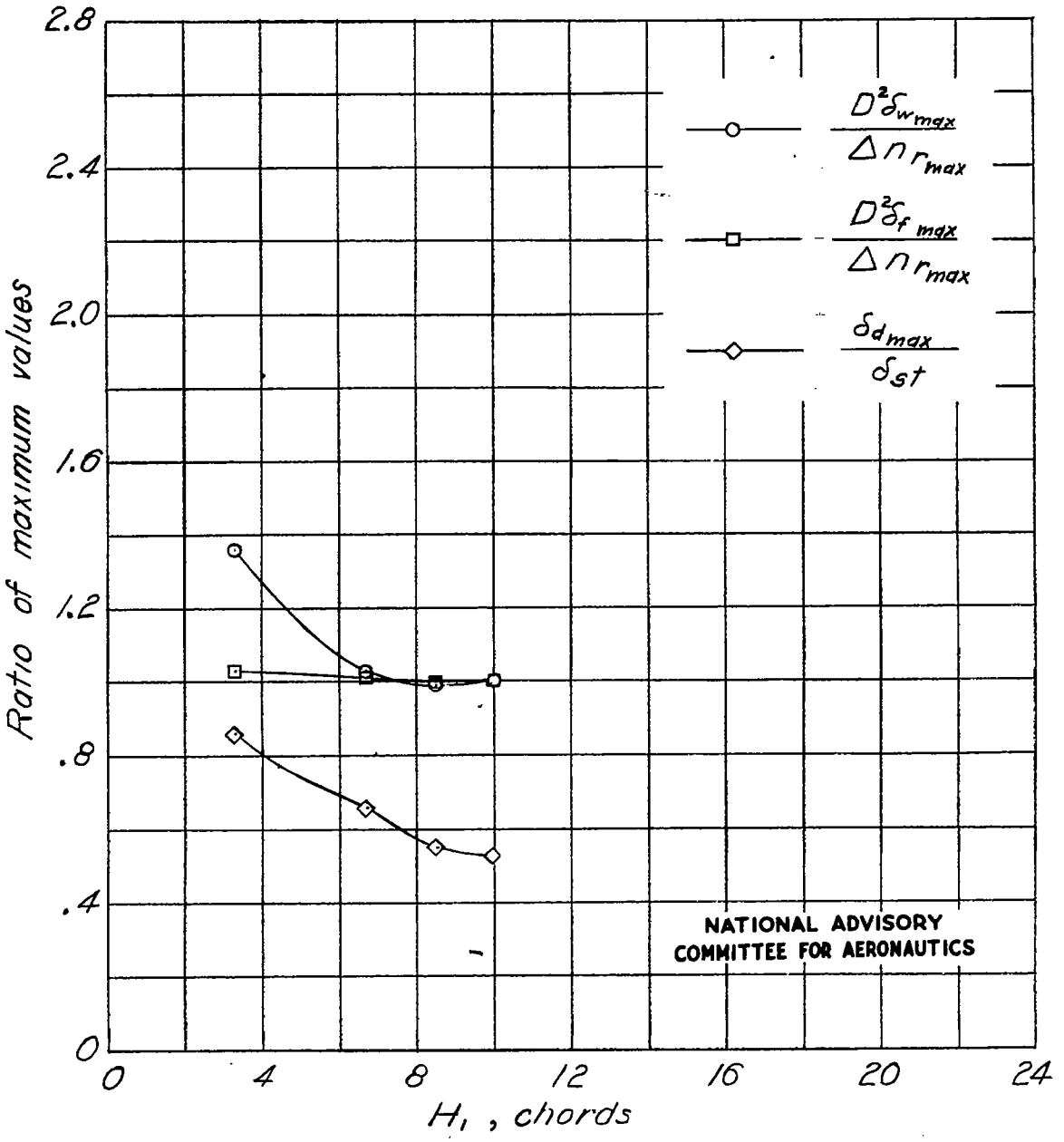

(d) Model B, condition 2

Figure 16.-Continued.

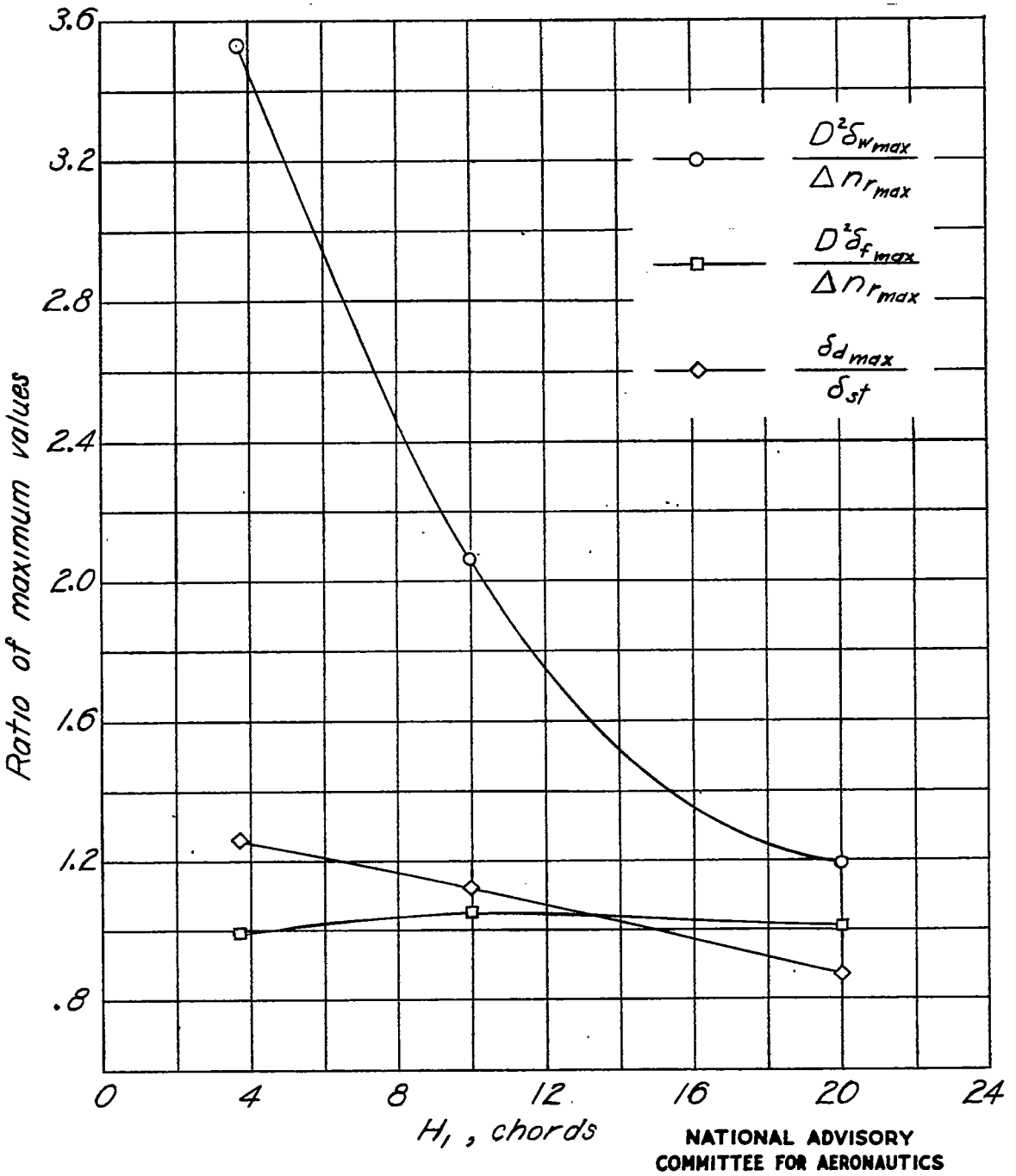

(e) Model C, condition 1.

Figure 16.-Continued.

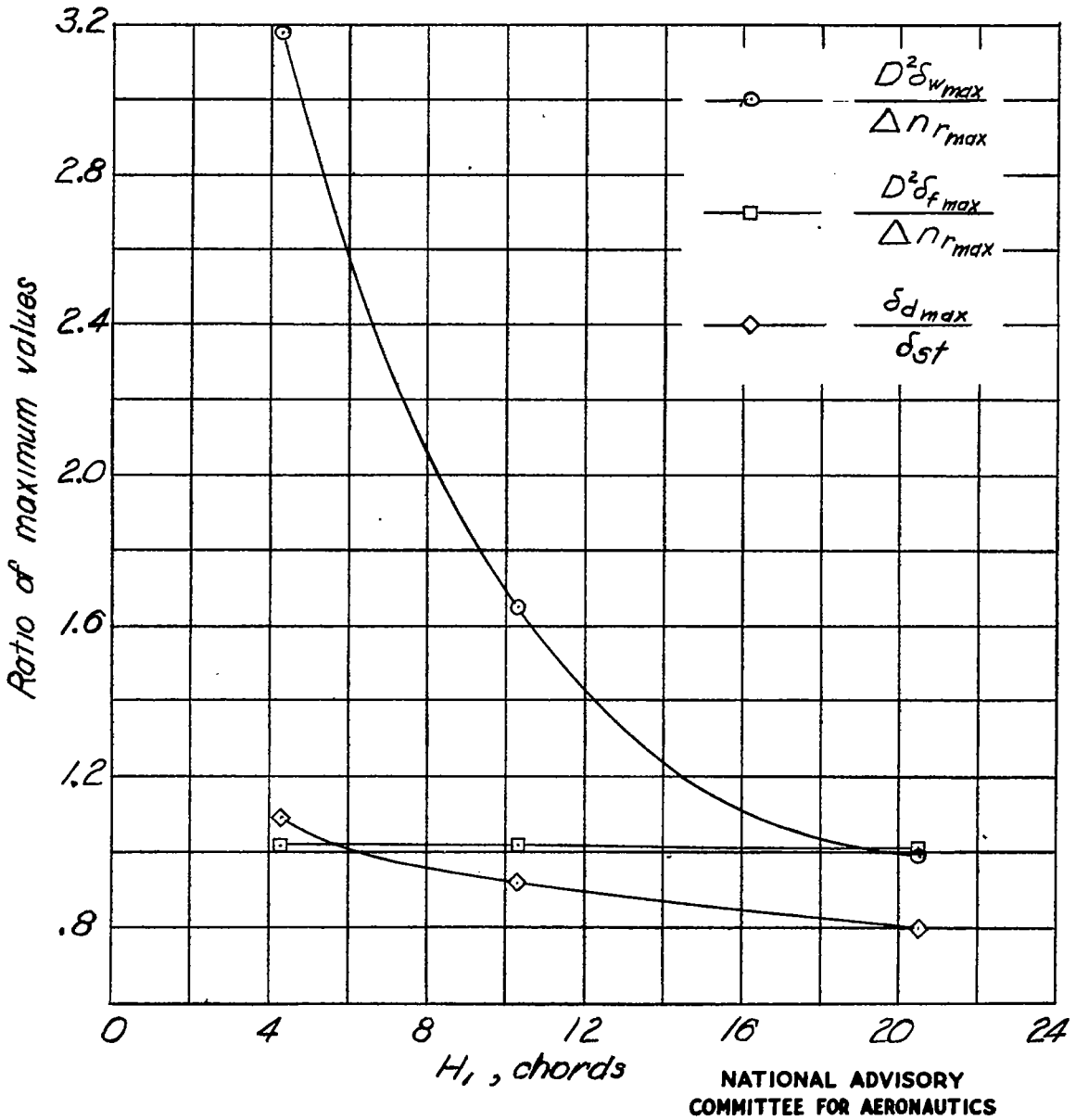

(f) Model D, condition 1.

Figure 16.-Continued.

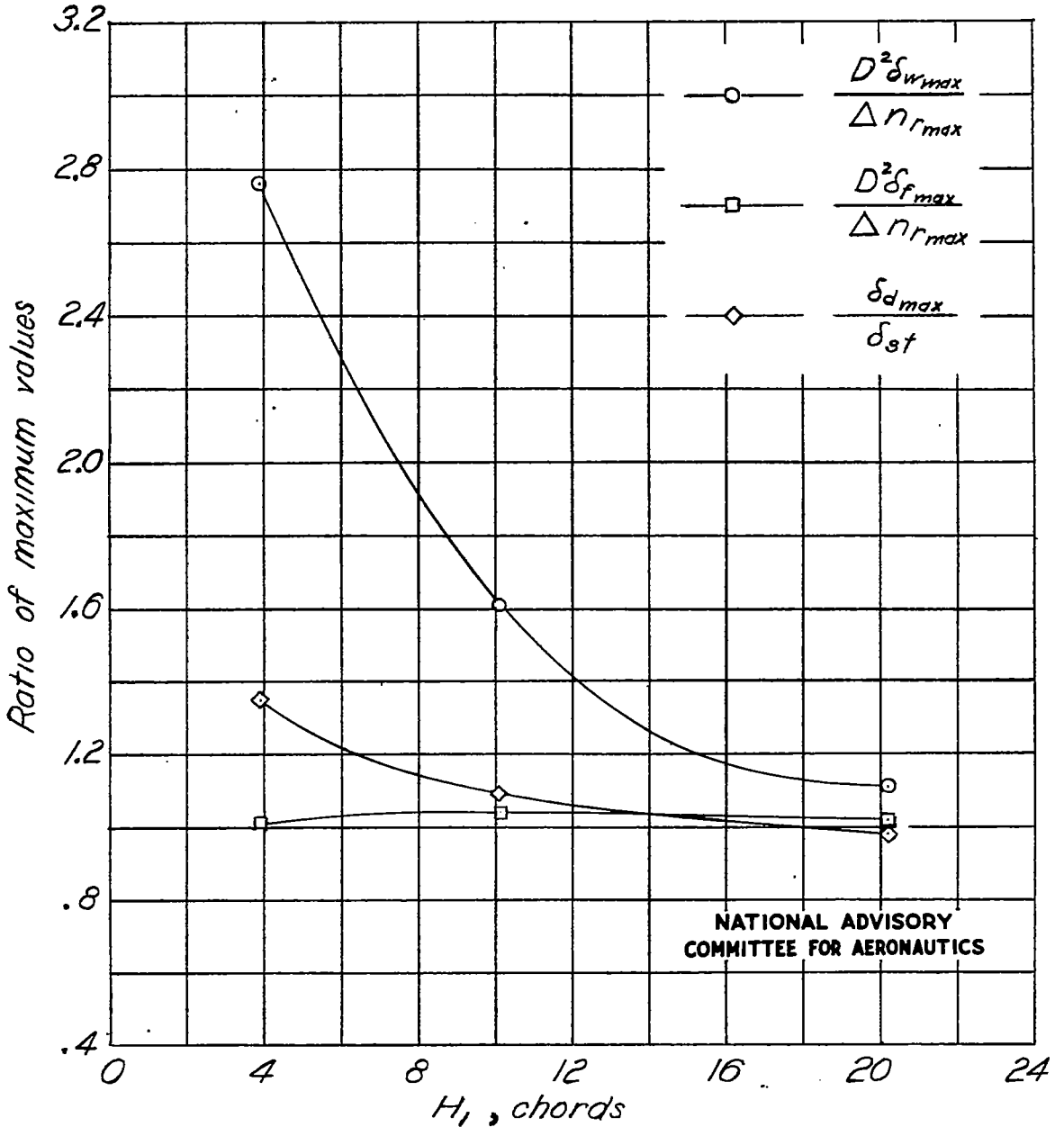

(g) Model D, condition 2.

Figure 16.- Concluded.

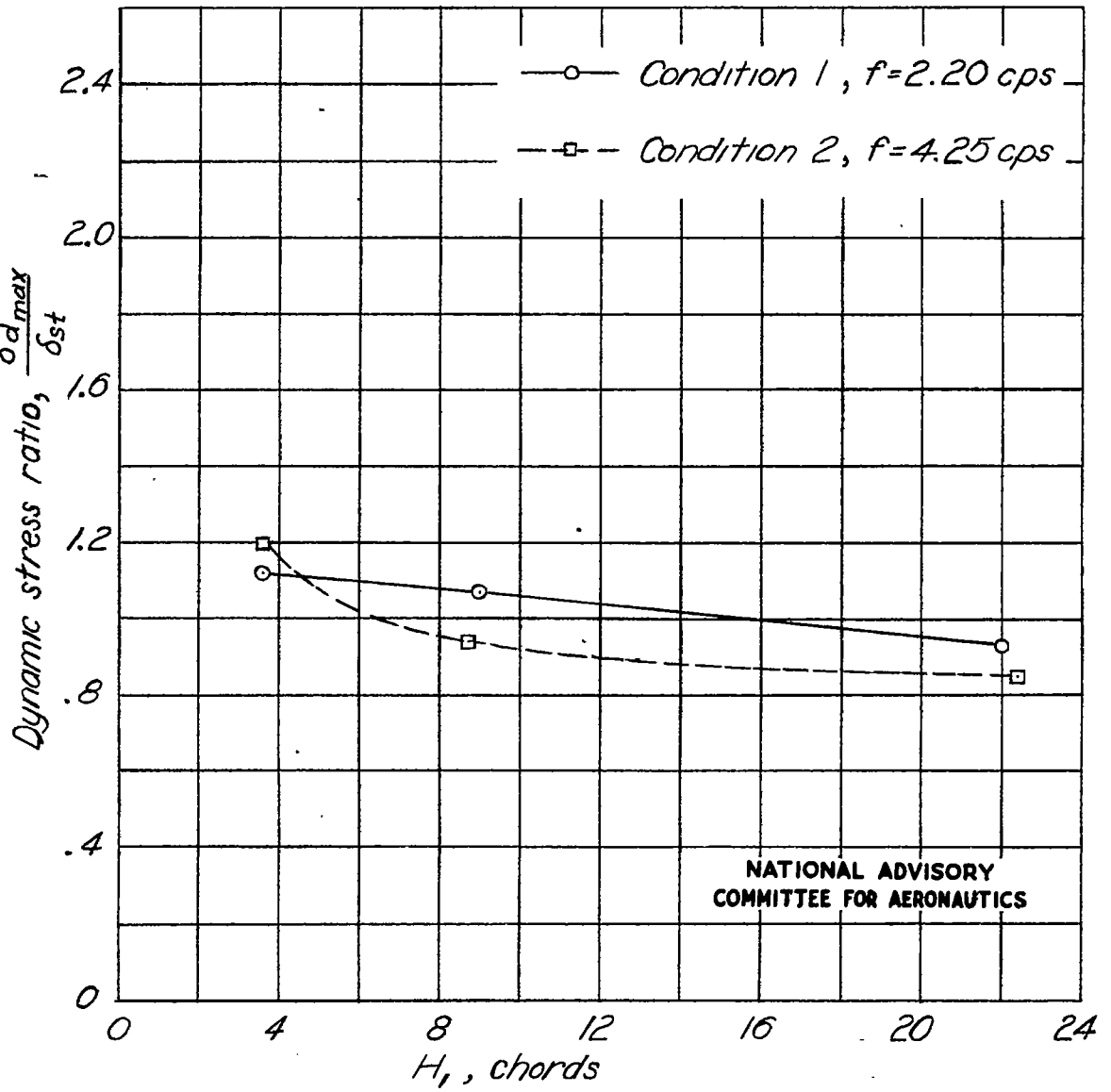

Figure 17.- Effect of change of wing frequency due to change of stiffness. Model A, conditions 1 and 2.

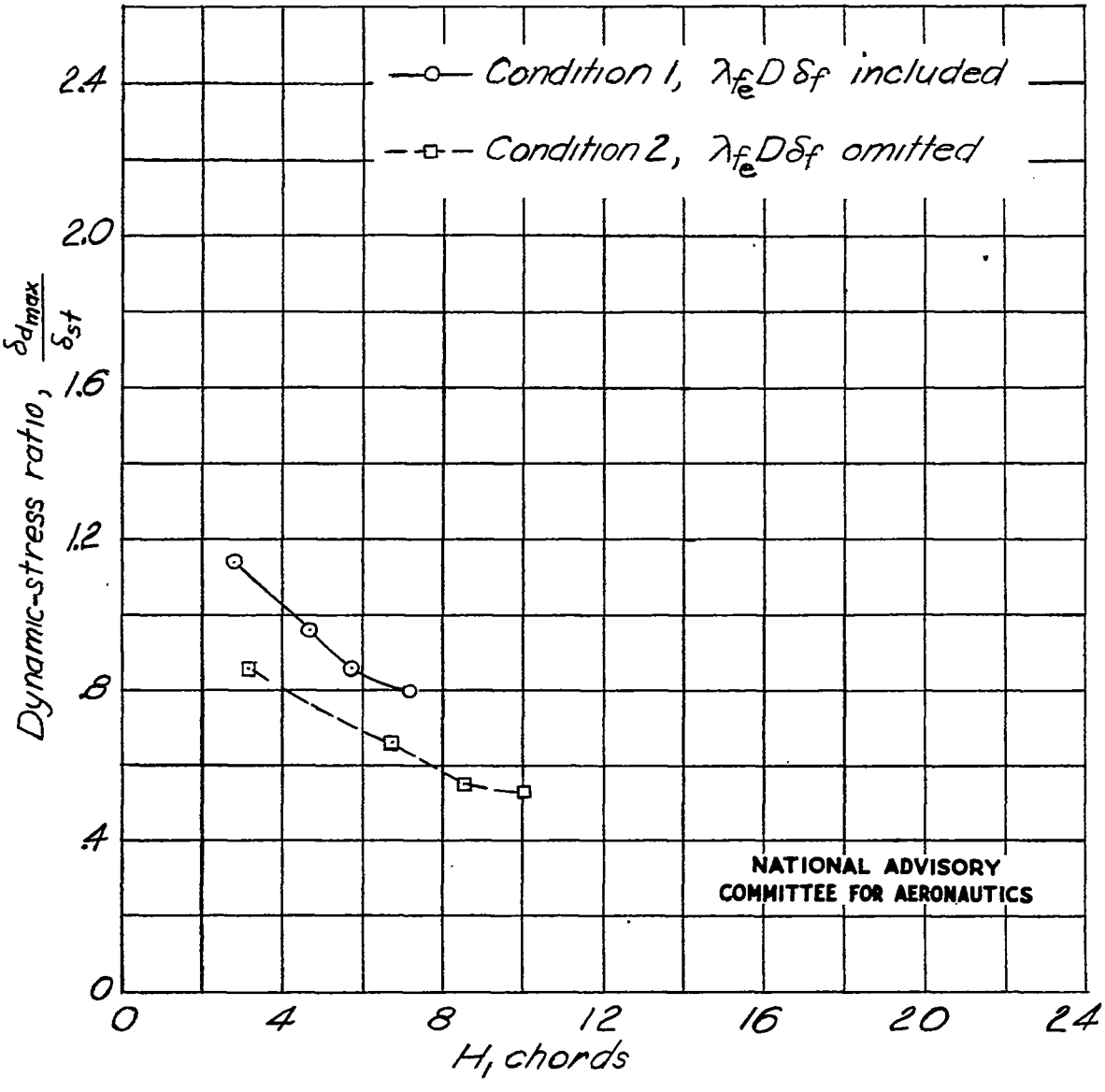

Figure 18.- Effect of omission of fuselage damping from calculation. Model B, conditions 1 and 2.

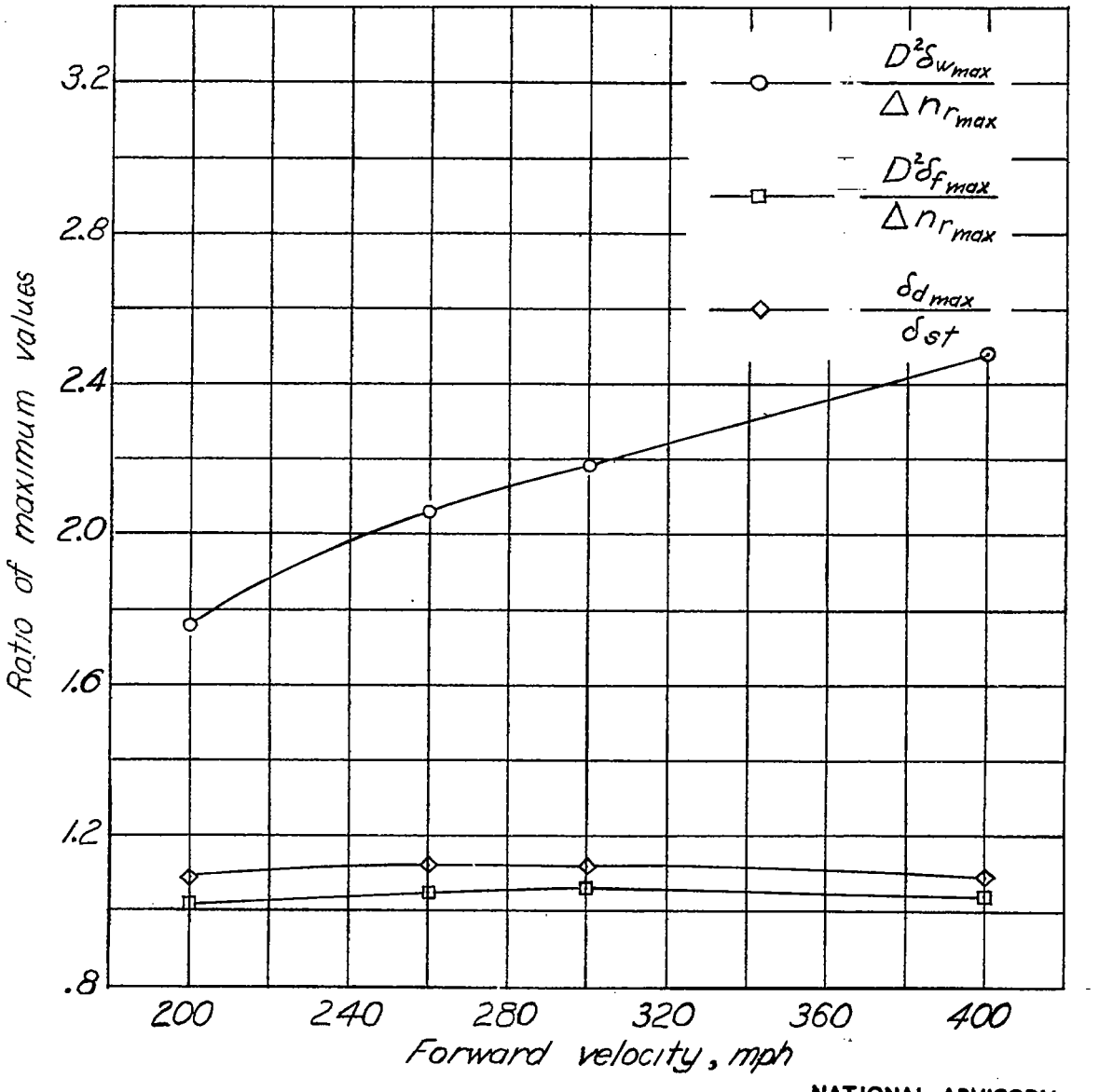

Figure 19.- Variations of ratios with change in forward velocity. Model C, conditions 1, 2, 3, and 4.

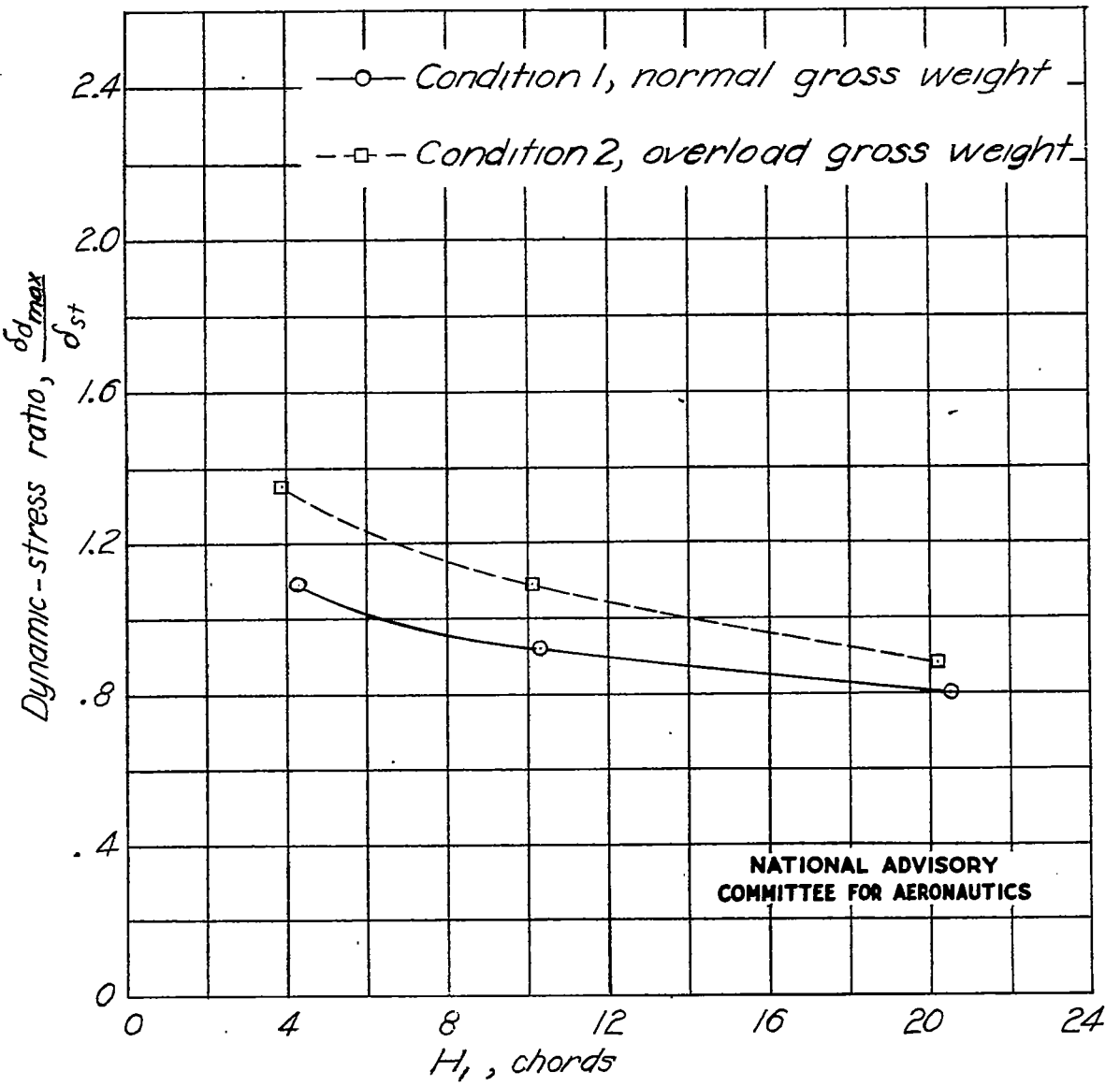

Figure 20.- Effect of change of wing frequency due to addition of mass. Model D, conditions 1 and 2.

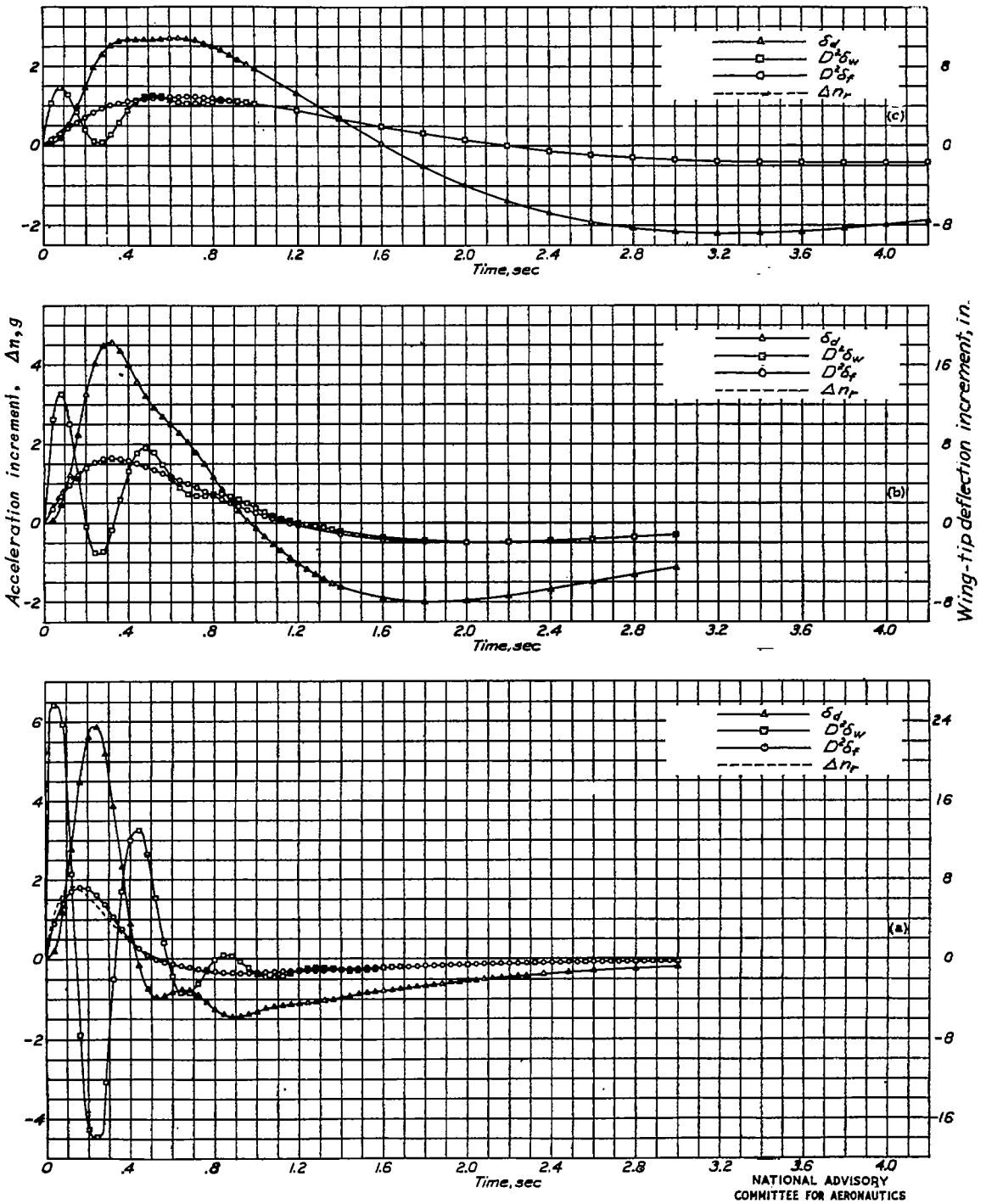

(a) H_1 = 3.75 chords; b = 0.94. (b) H_1 = 9.99 chords; b = 2.31. (c) H_1 = 19.98 chords; b = 0.887.

Figure 21. — Calculated history of reactions in a single gust. Model C, condition 1.

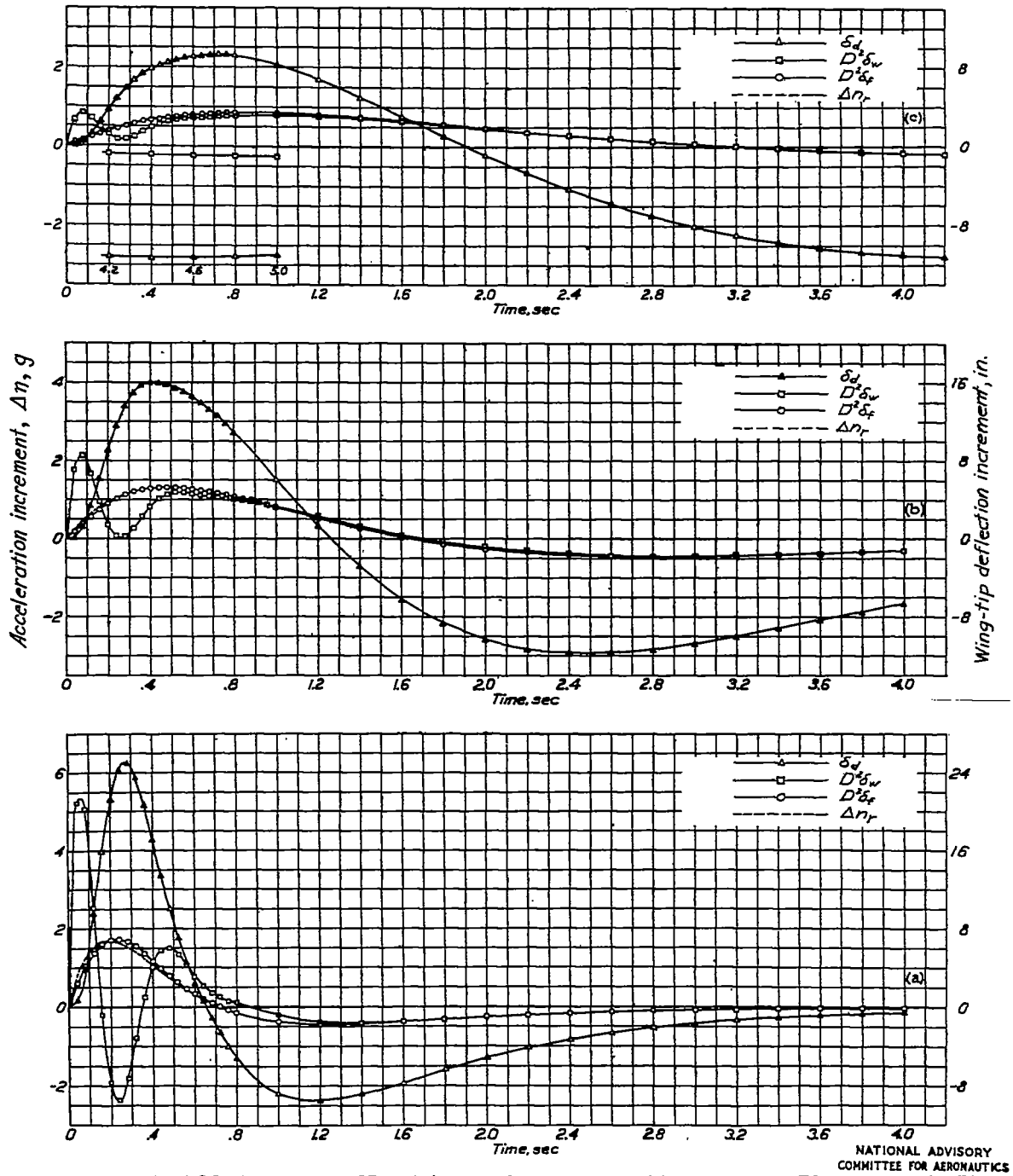

(a) $H_1 = 4.26$ chords; $b = 4.27$. (b) $H_1 = 10.25$ chords; $b = 1.26$. (c) $H_1 = 19.53$ chords; $b = 0.459$.

Figure 22.– Calculated history of reactions in a single gust. Model D, condition 1.

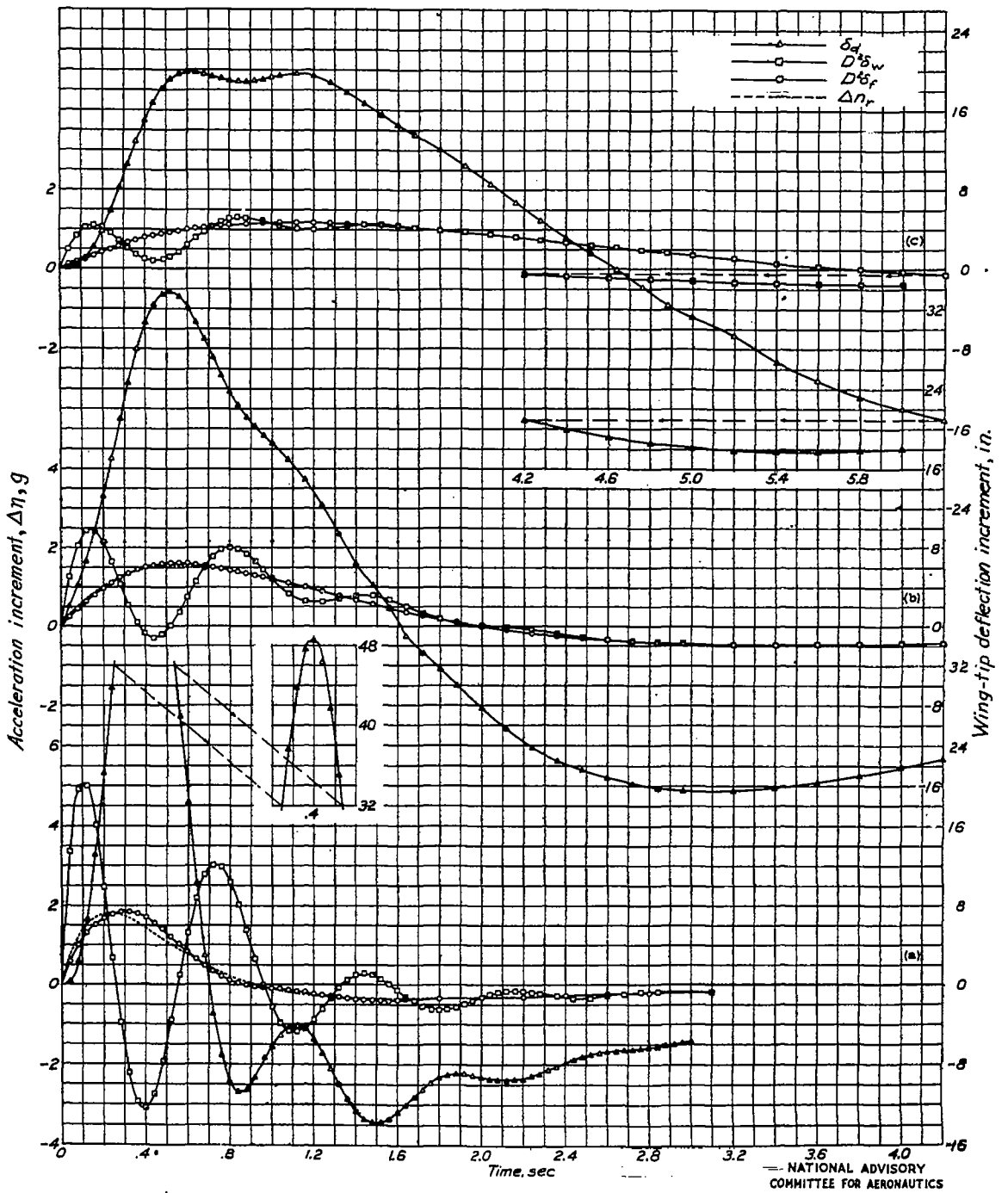

(a) $H_1 = 3.96$ chords; $b = 3.91$. (b) $H_1 = 10.08$ chords; $b = 1.30$. (c) $H_1 = 20.15$ chords; $b = 0.494$

Figure 23.- Calculated history of reactions in a single gust. Model D, condition 2.

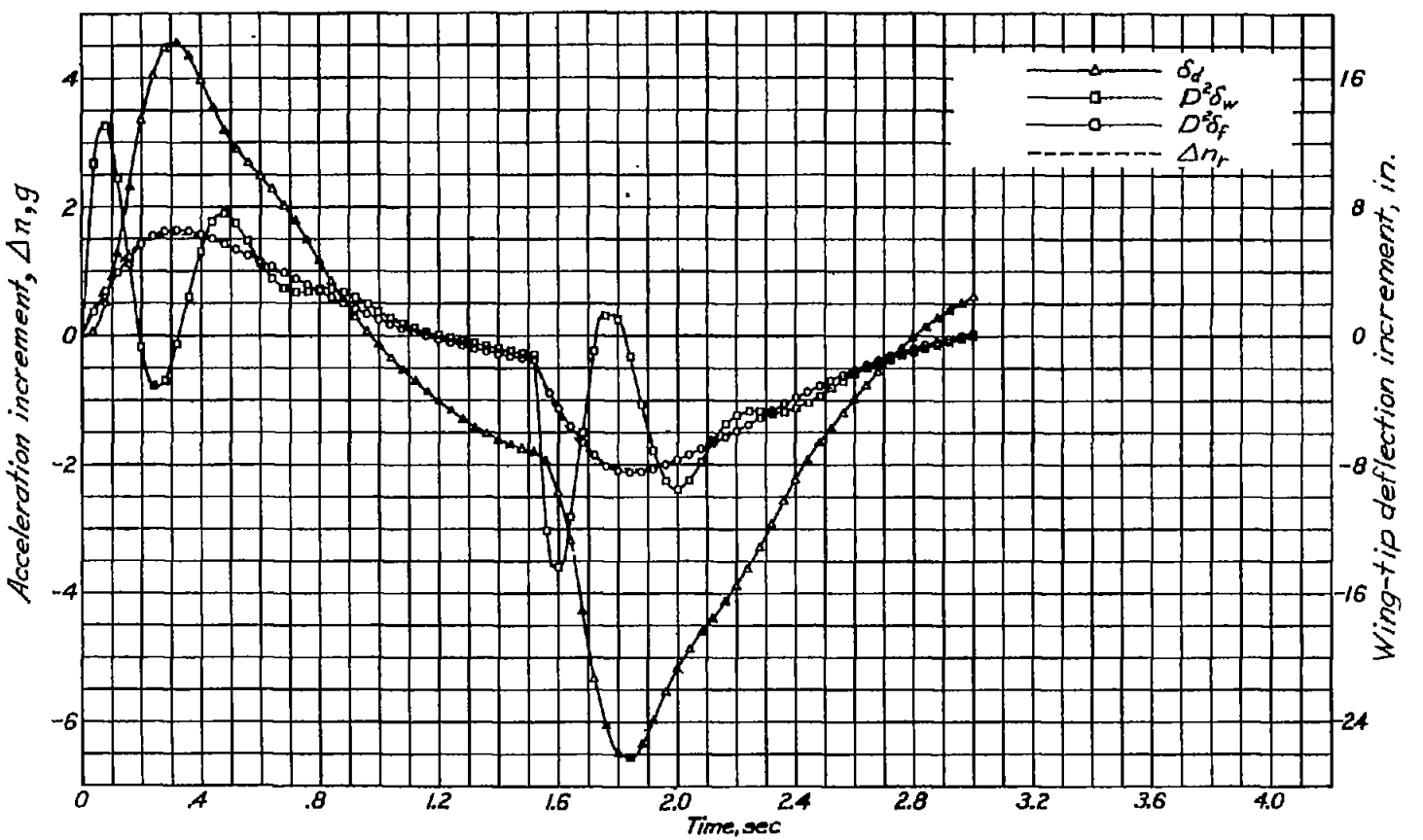

Figure 24. — Calculated history of reactions in a repeated gust. Model C, condition 1; $H_1 = H_2 = 9.99$ chords; $H_3 = 37.46$ chords; $U_2 = -U_1$.

NATIONAL ADVISORY COMMITTEE FOR AERONAUTICS

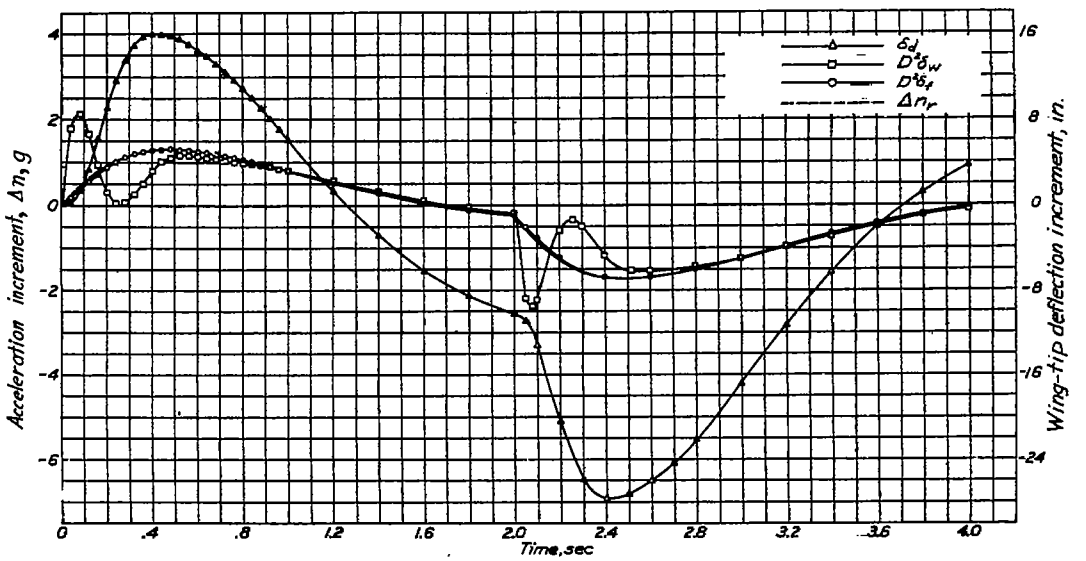

Figure 25.- Calculated history of reactions in a repeated gust. Model D, condition 1; $H_1 = H_2 = 10.25$ chords, $H_3 = 32.48$ chords; $U_2 = -U_1$.

NATIONAL ADVISORY COMMITTEE FOR AERONAUTICS

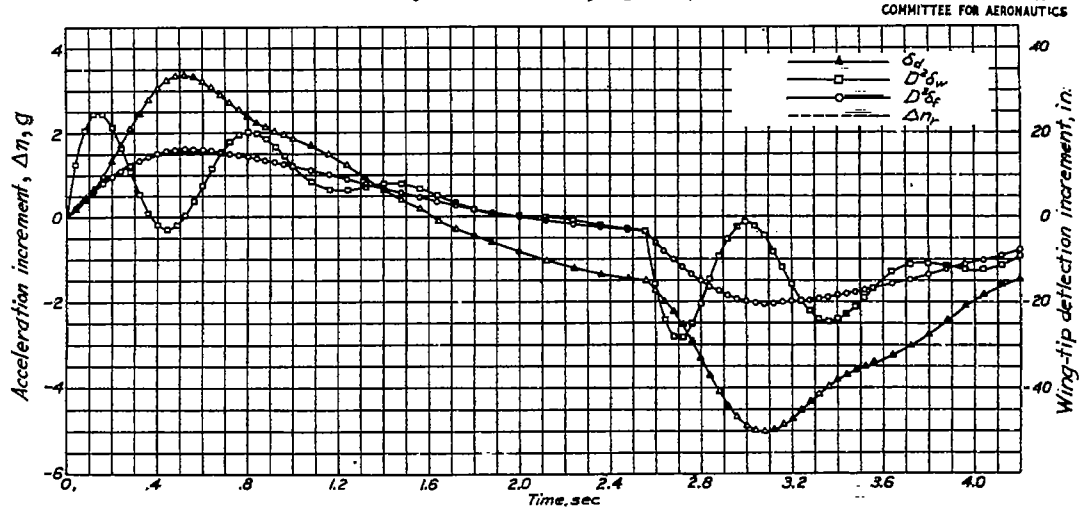

Figure 26.- Calculated history of reactions in a repeated gust. Model D, condition 2; $H_1 = H_2 = 10.08$ chords, $H_3 = 33.83$ chords; $U_2 = -U_1$.

NATIONAL ADVISORY COMMITTEE FOR AERONAUTICS